PHOTOGRAPH THIS SHEET

AD-A202 557

DTIC ACCESSION NUMBER

LEVEL

1

INVENTORY

AFATL-TR-88-95

DOCUMENT IDENTIFICATION

This document has been approved for public release and sale; its distribution is unlimited.

DISTRIBUTION STATEMENT

ACCESSION FOR	
NTIS	GRA&I
DTIC	TAB
UNANNOUNCED	
JUSTIFICATION	
BY	
DISTRIBUTION /	
AVAILABILITY CODES	
DIST	AVAIL AND/OR SPECIAL
A-1	

DISTRIBUTION STAMP

DTIC COPY INSPECTED

DTIC ELECTE AUG 19 1988 S D E

DATE ACCESSIONED

DATE RETURNED

88 8 19 013

DATE RECEIVED IN DTIC

REGISTERED OR CERTIFIED NO.

PHOTOGRAPH THIS SHEET AND RETURN TO DTIC-FDAC

DTIC FORM 70A MAR 86

DOCUMENT PROCESSING SHEET

PREVIOUS EDITION MAY BE USED UNTIL STOCK IS EXHAUSTED.

AFATL-TR-88-95

A Study of Transonic Drag Reduction of a Blunt Cylinder by a Cylinder Probe

David H Bridges

AERODYNAMICS BRANCH
AEROMECHANICS DIVISION

AUGUST 1988

FINAL REPORT FOR PERIOD OCTOBER 1985-JULY 1988

AIR FORCE ARMAMENT LABORATORY
Air Force Systems Command ▮ United States Air Force ▮ Eglin Air Force Base, Florida

NOTICE

When Government drawings, specifications, or other data are used for any purpose other than in connection with a definitly Government-related procurement, the United States Government incurs no responsibility nor any obligation whatsoever. The fact that the Government may have formulated or in any way supplied the said drawings, specifications, or other data, is not to be regarded by implication, or otherwise as in any manner construed, as licensing the holder, or any other person or corporation; or conveying any rights or permission to manufacture, use, or sell any patented invention that may in any way be related thereto.

The AFATL STINFO Officer has reviewed this report, and it is releasable to the National Technical Information Service (NTIS), where it will be available to the general public, including foreign nationals.

This report has been reviewed and is approved for publication.

FOR THE COMMANDER

Stephen C. Korn

STEPHEN C. KORN
Chief, Aeromechanics Division

Please do not request copies of this report from the Air Force Armament Laboratory. Copies may be obtained from DTIC. Address your request for additional copies to:

Defense Technical Information Center
Cameron Station
Alexandria, VA 22304-6145

If your address has changed, if you wish to be removed from our mailing list, or if your organization no longer employs the addressee, please notify AFATL/FXA, Eglin AFB, FL 32542-5434, to help us maintain a current mailing list.

Copies of this report should not be returned unless return is required by security considerations, contractual obligations, or notice on a specific document.

UNCLASSIFIED
SECURITY CLASSIFICATION OF THIS PAGE

REPORT DOCUMENTATION PAGE

Form Approved OMB No. 0704-0188

1a. REPORT SECURITY CLASSIFICATION UNCLASSIFIED	1b. RESTRICTIVE MARKINGS
2a. SECURITY CLASSIFICATION AUTHORITY	3. DISTRIBUTION/AVAILABILITY OF REPORT Approved for public release; distribution unlimited.
2b. DECLASSIFICATION/DOWNGRADING SCHEDULE	
4. PERFORMING ORGANIZATION REPORT NUMBER(S)	5. MONITORING ORGANIZATION REPORT NUMBER(S) AFATL-TR-88-95
6a. NAME OF PERFORMING ORGANIZATION Mississippi State University 6b. OFFICE SYMBOL (If applicable)	7a. NAME OF MONITORING ORGANIZATION Aerodynamics Branch Aeromechanics Division
6c. ADDRESS (City, State, and ZIP Code) Mississippi State MS 39762	7b. ADDRESS (City, State, and ZIP Code) Air Force Armament Laboratory Eglin Air Force Base, Florida 32542-5434
8a. NAME OF FUNDING/SPONSORING ORGANIZATION Aeromechanics Division 8b. OFFICE SYMBOL (If applicable) AFATL/FX	9. PROCUREMENT INSTRUMENT IDENTIFICATION NUMBER In-house
8c. ADDRESS (City, State, and ZIP Code) Air Force Armament Laboratory Eglin AFB FL 32542-5434	10. SOURCE OF FUNDING NUMBERS PROGRAM ELEMENT NO. 62602F; PROJECT NO. 2567; TASK NO 03; WORK UNIT ACCESSION NO. 05

11. TITLE (Include Security Classification)
A Study of Transonic Drag Reduction of a Blunt Cylinder by a Cylinder Probe

12. PERSONAL AUTHOR(S)
David H. Bridges

13a. TYPE OF REPORT	13b. TIME COVERED	14. DATE OF REPORT (Year, Month, Day)	15. PAGE COUNT
Final	FROM 8 Oct 85 TO 1 Jul 88	August 1988	57

16. SUPPLEMENTARY NOTATION
Availability of report is specified on verso of front cover.

17. COSATI CODES			18. SUBJECT TERMS (Continue on reverse if necessary and identify by block number)
FIELD	GROUP	SUB-GROUP	Experimental Aerodynamics, Cavity Flow, Favorable Interference
0101	1604	2004	

19. ABSTRACT (Continue on reverse if necessary and identify by block number)

The purposes of this study are to examine the reduction of the drag of a blunt cylinder by a cylindrical probe in the transonic regime, and to determine characteristics of the flowfield from the experimental drag coefficient data. This study is significant because it is the first extensive study of this flow in the transonic regime.

The experiment was conducted in the NASA-Ames Research Center 6 x 6 ft. supersonic wind tunnel. The model consisted of a blunt cylinder with diameter d_2 and several extendable cylindrical probes, yielding probe-to-cylinder diameter ratios d_1/d_2 of 0.248, 0.368, and 0.45, and probe length-to-cylinder diameter ratios $1/d_2$ up to 2.0 (3.0 for the smallest probe). These configurations were tested at Mach numbers between 0.8 and 1.5.

C_D decreased as both $1/d_2$ and d_1/d_2 increased, due to the fact that the cylinder face was immersed in a wake of reduced stagnation pressure created by the probe. After reaching a minimum, C_D increased as $1/d_2$ increased, indicating a transition of the flow over the probe from a lower-drag open cavity mode to a higher-drag closed cavity mode.

(continued)

20. DISTRIBUTION/AVAILABILITY OF ABSTRACT ☐ UNCLASSIFIED/UNLIMITED ☒ SAME AS RPT. ☐ DTIC USERS	21. ABSTRACT SECURITY CLASSIFICATION UNCLASSIFIED
22a. NAME OF RESPONSIBLE INDIVIDUAL LYNN M. LEWIS, JR	22b. TELEPHONE (Include Area Code) (904)882-3124 22c. OFFICE SYMBOL AFATL/FXA

DD Form 1473, JUN 86 *Previous editions are obsolete.*

SECURITY CLASSIFICATION OF THIS PAGE
UNCLASSIFIED

19. ABSTRACT (CONCLUDED)

This change was rather abrupt, and there was also hysteresis in the supersonic tests in agreement with previous experiments. C_D also reached a minimum and increased as d_1/d_2 approached 1.

C_D usually increased with Mach number due to the increase in stagnation pressure with M. For a particular range of length and diameter ratios, C_D decreased with increasing M for $0.8 < M < 0.95$. This was attributed to the transition of the flow over the probe from the higher-drag closed mode to the lower-drag open mode as M increased.

A STUDY OF THE TRANSONIC DRAG REDUCTION OF A BLUNT CYLINDER BY A CYLINDRICAL PROBE

by

David H. Bridges

A Thesis
Submitted to the Faculty of
Mississippi State University
in Partial Fulfillment of the Requirements
for the Degree of Master of Science
in the Department of Aerospace Engineering

Mississippi State, Mississippi

August 1987

A Study of the Transonic Drag Reduction of a Blunt Cylinder by a Cylindrical Probe

by

David H. Bridges

APPROVED

Professor of Aerospace Engineering and Head of Department

Director of Graduate Instruction, College of Engineering

Associate Professor of Aerospace Engineering (Major Professor)

Dean of the College of Engineering

Associate Professor of Aerospace Engineering (Departmental Graduate Coordinator)

Acting Associate Vice President for Academic Affairs

August 1987

ACKNOWLEDGMENTS

I would like to express my enormous gratitude to Dr. Keith Koenig, my major professor, for everything he has done and been for me in the years that I have known him. His teaching has been impeccable, his guidance invaluable, and his example one that I will not soon forget. Dr. Koenig, thank you.

I would also like to express my appreciation to the faculty and staff of the Aerospace Engineering Department. They have made my years as an undergraduate and graduate both educational and enjoyable, no easy feat.

Funds for the support of this study have been allocated by the NASA-Ames Research Center, Moffett Field, California, under Interchange No. NCA2-52. Funds for my graduate studies were provided by an Office of Naval Research Graduate Fellowship.

D.H.B.

Mississippi State University

August 1987

ABSTRACT

David H. Bridges, Master of Science, 1987

Major: Aerospace Engineering, Department of Aerospace Engineering

Title of Thesis: A Study of the Transonic Drag Reduction of a Blunt Cylinder by a Cylindrical Probe

Directed by: Dr. Keith Koenig

Pages in Thesis: 57 Words in Abstract: 283

ABSTRACT

The purposes of this study are to examine the reduction of the drag of a blunt cylinder by a cylindrical probe in the transonic regime, and to determine characteristics of the flowfield from the experimental drag coefficient data. This study is significant because it is the first extensive study of this flow in the transonic regime.

The experiment was conducted in the NASA Ames Research Center 6X6-ft. supersonic wind tunnel. The model consisted of a blunt cylinder with diameter d_2 and several extendable cylindrical probes, yielding probe-to-cylinder diameter ratios d_1/d_2 of 0.248, 0.368, and 0.45, and probe length-to-cylinder diameter ratios l/d_2 up to 2.0 (3.0 for the smallest probe). These configurations were tested at Mach numbers between 0.8 and 1.5.

C_D decreased as both l/d_2 and d_1/d_2 increased, due to the fact that the cylinder face was immersed in a wake of

reduced stagnation pressure created by the probe. After reaching a minimum, C_D increased as l/d_2 increased, indicating a transition of the flow over the probe from a lower-drag open cavity mode to a higher-drag closed cavity mode. This change was rather abrupt, and there was also hysteresis, in the supersonic tests, in agreement with previous experiments. C_D also reached a minimum and increased as d_1/d_2 increased, due to the increasing resemblance of the cylinder/probe configuration to a blunt cylinder as d_1/d_2 approached 1.

C_D usually increased with Mach number, due to the increase in stagnation pressure with M. For a particular range of length and diameter ratios, C_D decreased with increasing M for $0.8 < M < 0.95$. This was attributed to the transition of the flow over the probe from the higher-drag closed mode to the lower-drag open mode as M increased.

TABLE OF CONTENTS

LIST OF SYMBOLS

Symbol	
C_D	Drag coefficient
C_p	Pressure coefficient
d_1	Probe diameter
d_2	Cylinder diameter
l	Probe length
$(l/d_2)_{cr}$	Critical probe length ratio
M	Mach number
r_1	Probe radius
r_2	Cylinder radius
V	Freestream velocity

LIST OF FIGURES

I. INTRODUCTION

1.1 Description of Problem

The reduction of the drag of a blunt object by the use of a shielding device is a well-documented phenomenon[1-3], and the principle has been applied to vehicles ranging from tractor-trailer rigs[4,5] to the Trident missile[6]. This type of flow has been studied rather extensively in the incompressible[1] and supersonic[2,3] regimes. However, little attention has been paid to this flow in the transonic regime[7]. Only one experiment[6] has concentrated specifically on the transonic regime, and this experiment was limited to flow pictures and drag calculations from data obtained in a ballistics facility. No experiment has been conducted in the transonic regime that has compiled extensive force, pressure, and velocity data. To rectify this omission, an experiment was conducted in the National Aeronautics and Space Administration Ames Research Center (NASA-ARC) 6-foot supersonic wind tunnel. The model used was a blunt cylinder with a co-axial cylindrical probe extending ahead of the cylinder face. The axis of the model was aligned with the flow direction. The tunnel was run at freestream Mach numbers between 0.8 and 1.5. Force, pressure, and velocity measurements were made. This thesis is an examination of the drag data from this experiment, with the intention of determining various aspects of the flowfield from the drag data.

1.2 Background

The idea of using some sort of shielding device to reduce the drag of a blunt object seems to have first been explored by Eiffel[8] in his experiments on two discs in tandem. These experiments have been more recently repeated by Morel and Bohn[9]. Some of the earliest experiments involving the use of a probe to reduce the drag of a blunt, cylindrical object in the compressible regime were conducted by Spooner[2] and by Beastall and Turner[3]. Koenig[7] has compiled a fairly comprehensive survey of the work conducted prior to 1983 in the area of transonic merging separated flows and has explained how the results might be applied to the cylinder/probe drag reduction problem. The research by Haupt and Koenig[6] is one of the very few experiments to directly address the problem of the cylinder/probe configuration in transonic flow.

1.3 Qualitative Discussion of Drag Reduction and Flowfields

The geometry of interest in this thesis is shown in Figure 1. This configuration consists of a blunt cylinder of diameter d_2 with a cylindrical probe of diameter d_1 and length l aligned co-axially with the cylinder. The model used in the experiment was based on this configuration, and will be discussed in more detail later.

An examination of any of the data in the papers previously cited will reveal a decrease in the drag coefficient of the blunt cylinder - shielding device combination as the shielding device is extended in front of

the blunt cylinder. This shielding device usually takes the form of either a disc mounted on a probe or a probe with a blunt face. The decrease in drag is due to the fact that because of viscous forces, the flow that impacts on the disc or probe face separates from the edge of the disc or probe face, as sketched in Figure 2. This creates a large wake with reduced stagnation pressure in which the blunt cylinder face is immersed. The reduced stagnation pressure is the reason for decreased C_D. This is a reasonable explanation for the reduction of blunt body drag by a probe or disc. However, for a more complete description of the manner in which the flowfield affects the drag of the cylinder/probe configuration, it is necessary to include a brief discussion of cavity flows.

The similarities between the flow past the cylinder/probe combination and cavity flows has been well documented in the incompressible regime[10]. A comparison of the results of other experiments[2,6,7], as well as the data from the present experiment, with the incompressible results will confirm these similarities in the compressible regime. Of particular importance is the existence of the two cavity modes, open and closed (as defined by Charwat et. al.[11]), for the cylinder/probe configuration. Referring to Figure 3a, if the flow which separates from the probe face reattaches at the cylinder face, then the flow could be considered to be in the open cavity mode. If the flow that separates from the probe face reattaches on

the probe side, then separates again and reattaches on the cylinder face, as in Figure 3b, then the flow could be considered to be in the closed cavity mode. The existence of two modes is important because of the differences in drag experienced by the cylinder/probe configuration in the two different modes. For a given M and diameter ratio d_1/d_2, C_D is less for the open mode than for the closed mode. An examination of the pressure distribution in the cavity (as revealed by the pressure distribution along the probe side) for each of the two modes, as shown in Figure 3c, will reveal the reason for the drag difference. This figure is a qualitative sketch representative of the results of previous experiments on two-dimensional and axisymmetric cavities in incompressible and compressible flows[10-13]. The abscissa in this graph is the x-coordinate along the probe, with origin at the probe face corner, and nondimensionalized by the probe length. In both modes, the flow experiences an acceleration and sharp drop in pressure at the corner. In the closed mode, which occurs for "long" probes, the flow experiences a sharp recompression as it reattaches to the probe side and then another pressure rise as it separates ahead of the cylinder face. In the open mode for "short" probes, since the flow does not reattach to the probe side, it does not experience the sharp recompression. The open mode flow experiences only a gradual pressure rise as it approaches the cylinder face. The sharp recompression and the generally higher cavity

pressures in the closed mode lead to higher cylinder face pressures, and thus higher values of C_D, than for the open mode. This can be seen in several reports[3,6,7] which show that for flows that are known or can be assumed to be in the closed mode, C_D is higher than for the known or assumed open mode flows.

The mechanism which causes the cavity to close or open as the probe is lengthened or shortened is not well understood. The pressure distributions of Reference 10 seem to show that in the incompressible regime, the transition from one mode to another is very gradual, whereas the observations of Beastall and Turner[3] indicate that in the low supersonic regime ($1 < M < 2.5$), the change is rather abrupt. The observations of Beastall and Turner also demonstrate a hysteresis condition in the mode shape, with the probe length at which the mode changes (known as the critical length) being dependent upon whether the probe is being extended or retracted. Since the drag is dependent upon whether the cavity is open or closed, the abruptness of the mode transition and the hysteresis effects show up as sharp, clear hysteresis loops in the plots of C_D versus probe length for the supersonic Mach numbers. It should be noted that in the subsonic mode transition range, where the flow is undergoing the gradual transition from open to closed mode, the flowfield is very unsteady, with large fluctuations and large turbulent RMS velocities.

With this understanding of how features of the flowfield affect the drag of the cylinder/probe configuration, the experimental results may now be examined to yield information about characteristics of the flow past the cylinder/probe configuration.

II. EXPERIMENTAL DETAILS

2.1 Wind Tunnel

The tests were conducted in the NASA-ARC 6 X 6-ft supersonic wind tunnel. This is a closed circuit, single return, continuous flow tunnel powered by an 8-stage external axial compressor rated at 60000 hp. The Mach number is varied with an axisymmetric sliding block type nozzle. The test section is 6 feet high, 6 feet wide, and 14 feet long. It has a perforated ceiling and floor for transonic tests. The Mach number range of the facility is from M = 0.25 to M = 2.2, and the Reynold's number range is from 5 X 10^5 to 5 X 10^6 per foot. The tunnel stagnation pressure is variable from 4.4 to 14.7 psia, the tunnel dynamic pressure is variable from 200 to 1000 psf, and 580° R is the maximum tunnel stagnation temperature.

2.2 Model

The model was constructed according to the configuration shown in Figure 1, and consisted of a blunt cylinder with several extendable/retractable probes. The cylinder was made from aluminum and was 5 inches in diameter and 35 inches long. The cylinder face and side were instrumented with pressure taps. The usable face taps were located on a single radial line at radii of 1.25, 1.75, 2.0, 2.25, and 2.425 inches, measured from the centerline. The usable side taps were located at 1.25-inch intervals, beginning at the cylinder corner and

proceeding rearward along the cylinder side to 10 inches from the cylinder face, where the interval changed to 2.5 inches. This spacing continued until 15 inches from the cylinder face, where the interval changed again to 5 inches. The rearmost tap was 25 inches from the cylinder face. Thus, there were 13 usable taps on the cylinder side. There were also pressure taps located on the base of the cylinder and inside the cylinder cavity. These were used to measure base and cavity pressures, which were then used to compute a correction to the measured C_D that removed the base and cavity drag. The cylinder contained the drive mechanism for the extendable probes, and was mounted in the tunnel on a sting through a six-component internal balance. The balance was used to make force measurements.

There were essentially three different interchangeable probes used in the experiment. The first was an instrumented probe of diameter 1.84 inches, or $d_1/d_2 = 0.368$. This probe had pressure taps mounted on its face and side. The usable face taps were located on a single radial line at radii of 0.0, 0.465, and 0.736 inches, measured from the centerline. The usable side taps were located at 0.46-inch intervals from 0.92 inch behind the probe face to 5.52 inches behind the probe face, where the interval increased to 0.92 inches. The last tap was located 9.2 inches behind the probe face. There were 15 usable taps on the probe side. This probe could be

extended up to 10 inches (2 cylinder diameters) from the cylinder face.

There was a second, non-instrumented probe of diameter 1.24 inches, or d_1/d_2 = 0.248. This probe could be extended up to 10 inches (2 cylinder diameters) from the cylinder face. There was an extension that could be added to this probe so that it could extend up to 15 inches (3 cylinder diameters) from the cylinder face. The third probe was also non-instrumented. It was in fact a 1.24-inch diameter probe with a 2.25-inch diameter disc attached to the end, which yielded a diameter ratio d_1/d_2 of 0.45. This probe could also be extended up to 10 inches (2 cylinder diameters) from the cylinder face.

2.3 Data Acquisition

In addition to the force measurements made with the internal force balance and the pressure measurements made using the pressure taps, velocity data was also obtained. This was accomplished through the use of a two-component laser doppler velocimeter (LDV) system. This system measured mean velocity profiles, RMS velocity profiles, and turbulent shearing stress profiles. As is almost always the case with LDV data, the number of different cases covered was limited, and detailed pictures of the velocity field were obtained for only a few of the configurations and Mach numbers. Because of the limited scope of this set of data, it will not be included in this thesis.

2.4 Flow Regimes

The smallest probe (d_1/d_2 = 0.248) was tested over the range of Mach numbers 0.8 < M < 1.2 for the range of length ratios 0 < l/d_2 < 3. It was attempted to conduct these tests at a stagnation pressure equal to atmospheric pressure. However, due to difficulties with the tunnel, the tests were conducted at 1634 psf, approximately 77% of atmospheric pressure. The intermediate diameter probe (d_1/d_2 = 0.368) was tested over the range of Mach numbers 0.8 < M < 1.5 for the range of length ratios 0 < l/d_2 < 2. These tests were conducted with stagnation pressure equal to atmospheric. The probe-with-disc configuration (d_1/d_2 = 0.45) was tested for the range of Mach numbers 0.8 < M < 1.2. over the range of length ratios 0 < l/d_2 < 2. Again, because of difficulties with the tunnel, these tests were conducted at a stagnation pressure equal to 1634 psf (approximately 77% of atmospheric).

2.5 Other Details

As mentioned earlier, there were pressure taps located on the cylinder base and inside the cylinder cavity. These were used to compute the base drag of the cylinder, which was then used to correct the measured C_D. The reason that this correction was desired was that in these types of experiments, the greatest interest lies typically in the drag of the forebody system, which consists of the cylinder face and probe. This is because it is this part of the

geometry that causes C_D to vary the most. Thus, it is desired to determine the contribution to the total drag of the forebody system alone. The skin friction drag on the side of the cylinder is not corrected for because it contributes much less to the total drag than either the forebody system or the cylinder base.

In the discussion of the model construction, only the locations of the usable taps were noted. There were other pressure taps mounted on the cylinder and probe. However, these either duplicated the information given by the taps listed above or were determined to be unusable or bad at some point in the experiment, and so only the taps that yielded usable information were noted.

III. RESULTS

3.1 Variation of Drag Coefficient with Probe Length

Figures 4a through 4d show the variation of drag coefficient with probe length-to-cylinder diameter ratio (l/d_2) for each of the three different probe diameter ratios, with Mach number as the parameter between curves. Figures 4a and 4b contain the data for $d_1/d_2 = 0.248$ for the subsonic and supersonic Mach numbers, respectively, at which this probe was run. The subsonic and supersonic curves have been separated for clarity. Figures 4c and 4d contain the data for $d_1/d_2 = 0.368$ and $d_1/d_2 = 0.45$, respectively. Only the data for the extending probe lengths is shown in all cases except in Figure 4b, the supersonic drag curves for d_1/d_2. This is because in the cases where there was no hysteresis, the data for retracting probe lengths reasonably repeated the data for extending probe lengths, and so the repeated data points could be omitted for clarity.

As can be seen from these figures, all of the data begin with the same trend: a decrease in C_D as the probe length ratio increases from zero. This has been explained previously as being due to the reduced stagnation pressure of the flow impacting on the cylinder face. All of the subsonic drag curves show the same decrease in C_D until some sort of minimum is reached, and then C_D begins to increase gradually. This minimum appears to be at a probe length of roughly 1 cylinder diameter. Figure 4a shows the

trend for d_1/d_2 = 0.248 for a probe length extending to 3 cylinder diameters. C_D begins to increase slightly more rapidly in the range of probe lengths from 2 to 3 cylinder diameters. If the explanation given in the introduction is accepted, then the minimum and gradual rise in C_D indicates that the flow over the probe is transitioning from the open mode to the closed mode. The levelling off in the drag curves would indicate that the flow has completely transitioned to the closed mode. It appears in Figures 4c and 4d that C_D is beginning to increase for $l/d_2 > 1$, which would indicate that the flow in these two cases is beginning to transition to the closed mode.

The supersonic drag curves for d_1/d_2 = 0.368 and d_1/d_2 = 0.45 (Figures 4c and 4d) do not have a distinct minimum, but instead keep on decreasing for the entire range of length ratios investigated here. It should be noted that the drag curve for d_1/d_2 = 0.45, M = 1.2, appears to level off. However, it is possible that this is due to having a disc on the end of a probe instead of having just a blunt probe. Since no increase in drag is noted in the supersonic curves for these two probes, it would appear that the flow over these probes has not yet transitioned from open to closed mode for the length ratios shown. Figure 4b, on the other hand, contains abrupt drag rises and clear hysteresis loops for the larger values of l/d_2. In the hysteresis loops, the lower branch corresponds to increasing values of l/d_2, and the higher branch

corresponds to decreasing values of l/d_2. This would indicate that the flow undergoes an abrupt transition from open to closed mode as the probe is extended, and that the length ratio at which the mode transition occurs is dependent upon whether the probe is being extended or retracted, as discussed in the introduction.

Another important feature to note on these figures is the point or points at which the curves for the subsonic flows cross, and the point or points at which the curves for the supersonic flows cross. For $d_1/d_2 = 0.368$ (Figure 4c), the point on the subsonic curves is at a probe length of approximately 1.6 cylinder diameters, and on the supersonic curves, at a probe length of approximately 0.8 cylinder diameter. For $d_1/d_2 = 0.45$ (Figure 4d), the point on the subsonic curves is at a probe length of approximately 1.6 cylinder diameters, and on the supersonic curves, at a probe length of approximately 1 cylinder diameter. For the subsonic curves for $d_1/d_2 = 0.248$ (Figure 4a), there are two crossings: one at a probe length of approximately 1.6 cylinder diameters, and another at approximately 2.4 cylinder diameters. For the supersonic curves for $d_1/d_2 = 0.248$ (Figure 4b), there is one distinct crossing at a probe length of approximately 0.9 cylinder diameter. These crossings are important because they define limits for ranges of probe length ratios within which some peculiar variations of C_D with Mach number

occur. These variations will be discussed in a later section.

3.2 Variation of Drag Coefficient with Diameter Ratio

Figures 5a through 5f show examples of the variation of C_D with diameter ratio (d_1/d_2). Each figure contains the drag curves for all of the Mach numbers and for a particular probe length ratio. These curves were obtained in the following manner. For a particular length ratio and Mach number, the values of drag coefficient were obtained for the three different configurations, i. e., for the diameter ratios of 0.248, 0.368, and 0.45. Two other values were obtained in order to extend the domain of the curves. In the limits of $d_1/d_2 = 0$ and $d_1/d_2 = 1$, the cylinder/probe configuration reduces to a blunt cylinder. For the zero diameter ratio case, the configuration is exactly the same as the model cylinder with zero probe extension, and so the measured C_D for the model cylinder with zero probe length at the particular Mach number was used. For $d_1/d_2 = 1$, the configuration is also a blunt cylinder, but longer, by the probe length, than the model cylinder. Therefore, for this case, a slight increment was added to the measured C_D for the cylinder with zero probe length at the particular Mach number, to take into account the increase in drag due to skin friction. This increment was calculated by using an expression from White[14] to give the skin friction coefficient for the cylinder in incompressible flow, and then correcting this value

according to the data in Chapman and Kester[15], which documents the change in skin friction coefficient of a cylinder with Mach number. The increment in C_D was calculated assuming that this corrected C_f acted over a cylinder segment equal to the probe length. Thus, five actual data points were available for each length ratio and Mach number. The curves shown in Figures 5a through 5f were obtained from a cubic spline curvefit through these five data points.

Figure 5a contains the drag curves for $l/d_2 = 0.1$. This figure indicates that at this small length ratio the variation of diameter ratio has little effect on the drag. This is probably because for this small probe length, the probe is having very little effect on the flow impacting on the cylinder face. Figure 5b contains the drag curves for $l/d_2 = 0.3$. In this figure, the effect of increasing diameter ratio can clearly be seen. As the diameter ratio increases, C_D initially decreases to a minimum for all of the Mach numbers. This is probably due to the increased size of the separated region, or wake, with reduced stagnation pressure, that acts on the face. The reason for the slightly more negative slope for $0.368 < d_1/d_2 < 0.45$ is unclear. It is possible that this change in slope is due to use of a disc on a small probe, rather than a solid probe, to obtain a diameter ratio of 0.45, as mentioned previously. With the disc, there would be a greater chance of "trapping" a vortex between the disc and the cylinder

face, at the smaller length ratios, than with the probe alone. The vortex would lower the cylinder face pressures, thus decreasing C_D. This type of flow has produced remarkable drag reductions in the incompressible regime[1]. Eventually, the C_D curves reach a minimum, and then begin to increase with increasing diameter ratio. This is due to the fact that as the diameter ratio increases, there is a larger blunt face on the probe exposed to the oncoming flow, and hence a larger region over which near-stagnation pressures can act, leading to a higher C_D. The same trends continue for the other length ratios, with the portion of the curve with a more negative slope tending to disappear as the length ratio is increased. This would support the supposition that this "kink" in the drag curves is a disc effect, since the differences between a blunt probe and a probe with a disc would disappear as the probe got longer. This would be especially true once the flow transitioned to the closed mode, since the only effect of the disc would be to create a slightly larger separated region than would otherwise normally exist.

As with the C_D-versus-l/d_2 curves discussed earlier, there are some ranges of diameter ratios in which C_D exhibits some peculiar variations with Mach number. Again, these ranges have limits at the points where the drag curves for various Mach numbers cross. Since there are no actual data points for $0.45 < d_1/d_2 < 1.0$, in this region, only crossings that are indicated by the values at $d_1/d_2 =$

0.45 and $d_1/d_2 = 1$ will be noted, and values of the diameter ratio for the crossing points in this region will not be given. Crossings for $d_1/d_2 < 0.45$ will be referred to as actual crossings, while crossings for $0.45 < d_1/d_2 < 1.0$ as described above will be referred to as indicated crossings.

For the two smallest length ratios, no actual nor indicated crossings exist. For $l/d_2 = 1.0$ (Figure 5d), there are actual crossings in both the subsonic and supersonic drag curves at d_1/d_2 approximately equal to 0.2, and another actual crossing in the supersonic drag curves at d_1/d_2 approximately equal to 0.45. For $l/d_2 = 1.5$, there are two actual crossings each in both the subsonic and supersonic drag curves. The crossings in the subsonic drag curves occur at d_1/d_2 approximately equal to 0.3 and 0.45, and the crossings in the supersonic drag curves occur at d_1/d_2 approximately equal to 0.1 and 0.45. For a length ratio of 2, there are an actual and an indicated crossing in the subsonic drag curves, and two actual crossings in the supersonic drag curves. The actual crossing in the subsonic curves occurs at d_1/d_2 approximately equal to 0.15, and the two actual crossings in the supersonic drag curves occur at d_1/d_2 approximately equal to 0.06 and 0.42. The importance of these crossings will be discussed later.

3.3 Drag Coefficient Contours

Figures 6a through 6f are contour plots for various values of C_D, each plot containing the data for a different

Mach number. These figures show the combinations of length ratio and diameter ratio that have the same value of C_D for a given Mach number. These figures were created by constructing curves such as those shown in Figure 5 for all of the length ratios studied. The cubic spline equations were used to obtain values of C_D on a uniform grid of diameter and length ratios. This grid was then used by a plotting program to generate the contour plots.

Two important points may be noted from these figures. It appears that the minimum C_D occurs over a small but usuable range of length and diameter ratios. C_D also appears to be relatively insensitive to the length ratio beyond a certain value of l/d_2.

Because of the use of many interpolated points in these figures, they should be used only to gain a qualitative understanding of the flow features, and not to obtain precise quantitative characteristics of the flow.

3.4 Variation of Drag Coefficient with Mach Number

Figures 7a through 7d are examples of the variation of C_D with Mach number. Each figure contains the curves for a particular diameter ratio and for several length ratios for which that diameter ratio was tested.

The results that might have been expected will be discussed first. The most common trend, and the one that was most expected, was the increase in C_D in the range $0.95 < M < 1.1$ for all of the geometries tested. This can be attributed to the phenomenon of transonic drag rise, which

is usually caused by a rise in stagnation pressure as M increases and shock wave-boundary layer interactions. For the small length ratios (l/d_2 nominally less than 1), the drag coefficient increases with Mach number for the entire range of Mach numbers and diameter ratios tested. This indicates that for these small length ratios, the cylinder/probe configuration behaves essentially as a blunt cylinder, whose drag coefficient continues to rise with increasing Mach number because of the rise in stagnation pressure of the flow, due to compressibility.

For the two smaller diameter ratios, C_D decreases with increasing Mach number in the range $M > 1.1$ for most of the length ratios tested, while for the largest diameter ratio, C_D increases for $M > 1.1$. The decrease in C_D with increase in M in the supersonic regime for streamlined bodies is well documented[16,17]. This would indicate that in the supersonic regime, the separated flow over the cylinder/probe configurations with the smaller diameter ratios is essentially giving a streamlined shape to the body, which then leads to the decrease in C_D with increase in M. In the case of the largest diameter ratio, it would appear that the large probe face is the dominating feature. The large probe face causes the cylinder/probe combination to behave essentially as a blunt cylinder in the supersonic regime, with C_D rising as the stagnation pressure rises with Mach number.

Note that in the supersonic regime, for small length ratios (nominally less than 0.8) and all diameter ratios, C_D increases with increasing M, whereas for the larger length ratios (nominally greater than 1) and the two smaller diameter ratios, C_D decreases with increasing M. It would appear that there is some sort of transition from a "blunt cylinder" mode to a "streamlined" mode at some particular length ratio for the two smaller diameter ratios. This transition occurs at the first crossing of the supersonic drag curves in Figures 4b and 4c. This transition is even more graphically depicted in the supersonic drag curves of Figures 5d through 5f, in which the crossings indicate a transition from the blunt mode to the streamlined mode and back to the blunt mode as the diameter ratio increases from 0 to 1 for the larger length ratios.

One other expected trend was the increase in C_D with increasing M in the range $0.8 < M < 1.1$ for $d_1/d_2 = 0.248$ and $2.5 < l/d_2 < 3.0$. Since in this range of length ratios and Mach numbers the flow is essentially in the closed mode and no further significant changes in the flowfield are expected, the rise in C_D can be attributed once again to the increase in stagnation pressure with Mach number.

There were also two unexpected trends in the data. The most significant of these was the <u>decrease</u> in C_D with increasing Mach number in the range $0.8 < M < 0.95$ for all of the diameter ratios tested and for a certain range of

length ratios for each diameter ratio. While this type of drag reduction has been recorded before[15], it apparently has not received much attention. This phenomenon may be understood by a consideration of the transisiton of cavities from open to closed mode and the probe length ratio at which this transition occurs, known as the critical length ratio $(l/d_2)_{cr}$.

As explained in the introduction, as the probe gets longer, the flow past the probe transitions from the open cavity mode to the closed cavity mode. In the subsonic regime, this transition is gradual, and leads to a gradual increase in C_D. Because of the gradual transition, it is difficult to precisely determine a critical probe length ratio. However, it is possible to define a critical length ratio as that length ratio at which the drag coefficient is the average of the drag levels in the open and closed modes. Using this definition for the supersonic regime also, Figure 8 was constructed to show the variation of $(l/d_2)_{cr}$ with Mach number for $d_1/d_2 = 0.248$. This figure is limited to this diameter ratio because length ratios at which the flow had fully transitioned to the closed mode were obtained only with this diameter ratio. The figure was constructed by plotting each of the curves in Figures 4a and 4b separately, choosing two distinct drag levels, finding the midpoint between these two levels, and then recording the length ratio at which the average C_D occured. The definition of critical length and its implementation in

this procedure are somewhat subjective but yields at least qualitative information about the variation of critical probe length ratio with Mach number. As can be seen in Figure 8, $(l/d_2)_{cr}$ increases with increasing subsonic Mach number, and decreases with increasing supersonic Mach number for both the probe extending and retracting cases. It is this variation of $(l/d_2)_{cr}$ that explains the drop in C_D with increasing M for the subsonic case. For a fixed length ratio in the range of length ratios for which the drop in C_D occurs, it appears that the flow is in the higher drag closed mode for M = 0.8; i. e., $(l/d_2)/(l/d_2)_{cr} > 1$ at this Mach number. As M increases (below M = 1), $(l/d_2)_{cr}$ increases, so that $(l/d_2)/(l/d_2)_{cr}$ decreases until it becomes less than 1, and the flow transitions from the closed mode to the lower drag open mode. In other words, increasing the Mach number for a fixed length ratio in the proper range opens the cavity, thus reducing the drag. The range of length ratios for which this phenomenon occurs is indicated by the crossings in the subsonic drag curves in Figures 4a, 4c, and 4d, so that the significance of these crossings is demonstrated. The range of diameter ratios for which this phenomenon occurs is indicated by the crossings in the subsonic curves of Figures 5a through 5f, which seem to indicate that the range of diameter ratios chosen for this experiment just happened to coincide with the range of diameter ratios for which this phenomenon would occur.

The variation in critical probe length with Mach number also explains the other unexpected trend, which is an increase in C_D with increasing M in the range $1.1 < M < 1.2$ for some of the length ratios. For a fixed probe length ratio in the range of length ratios for which this phenomenon occurs, it appears that the flow is in the lower drag open mode for $M = 1.1$; i. e., $(l/d_2)/(l/d_2)_{cr} < 1$ at this Mach number. As the Mach number increases, $(l/d_2)_{cr}$ decreases, so that $(l/d_2)/(l/d_2)_{cr}$ increases until it becomes greater than 1, and so it appears that the flow transitions from the lower drag open mode to the higher drag closed mode. In other words, increasing the Mach number closes the cavity, and hence raises C_D. Due to the hysteresis of the supersonic drag curves in Figure 4b, it is a bit more difficult to determine the ranges of length ratios for which this phenomenon occurs. Examining Figure 4b, it would seem that the range is defined by the length ratios where the low drag branch of the $M = 1.1$ curve is below the high drag branch of the $M = 1.2$ curve, i. e., from nominally 1.8 to 2.2 cylinder diameters. Once the length ratio is reached at which both the $M = 1.1$ flow and the $M = 1.2$ flow have transitioned fully to the closed modes, the trend of decreasing C_D with increasing supersonic M returns.

Figure 7c indicates a rise in C_D as the Mach number increases from 1.2 to 1.5 for $d_1/d_2 = 0.368$, an unexpected trend in light of the observations concerning supersonic

drag characteristics presented earlier. Because of the lack of data for the other configurations at M = 1.5 (most notably for the longer probe ratios), it is difficult to draw conclusions about this trend. One possible explanation is that this increase is due to the increase in stagnation pressure with Mach number, so that for the higher Mach number, the cylinder/probe configuration at this diameter ratio is beginning to behave as a blunt cylinder.

3.5 Computed Drag Coefficients

Cylinder face pressure distributions were available for all of the configurations and Mach numbers. Probe face pressures were available for d_1/d_2 = 0.368. Using these pressures and some estimate of the skin friction on the cylinder, it should be possible to compute the drag coefficient of the cylinder/probe configuration, and this C_D should equal the measured C_D (within the range of experimental error). Figures 9a and 9b are examples of the results of such calculations.

Two pressures important to the calculations, the probe face corner pressure and the cylinder face corner pressure, were not available, so estimates had to be made for these two pressures. It was assumed that the outermost cylinder face pressure (measured at 0.075 inches from the cylinder corner) was the corner pressure. The probe face corner pressure estimate was a little more complicated. For zero probe length, the pressure was assumed to be an average of

the outermost probe face pressure and the innermost cylinder face pressure. For large probe lengths ($l/d_2 > 1$), the pressure was assumed to be the critical pressure, i. e., the value the pressure would have if the flow over the probe face corner was sonic. For $0 < l/d_2 < 1$, an average between these two estimated pressures, weighted by the probe length, was used. Another pressure, the cylinder face pressure immediately adjacent to the probe side, was also unavailable. This value was assumed to be equal to the innermost cylinder face pressure, a not unreasonable assumption considering the typically constant pressures in this region. The drag coefficient due to the skin friction was calulated using the method described in Section 3.2, assuming this C_f acted over 80% of the cylinder. The other 20% was assumed to be effectively canceled by the reversed flow and hence reversed-direction skin friction coefficients acting in the recirculating region immediately behind the cylinder face.

Figures 9a and 9b were constructed by calculating separately the contributions to the drag coefficient of the probe face, cylinder face, and cylinder side (the contribution of the probe side was assumed to be zero). The cylinder side (skin friction) curve, labelled "C_{Dcs}", was plotted first. The cylinder side and cylinder face drag coefficients were added together and plotted as the curve labelled "C_{Dcf}". The cylinder side, cylinder face, and probe face drag coefficients were added together and

plotted as the curve labelled "C_{Dpf}". This curve represents the sum of all of the computed drag coefficients.

In Figures 9a and 9b, the curve labelled "C_{Dm}" is the measured C_D curve. The "C_{Dpf}" and "C_{Dm}" curves should match one another, within the range of experimental error. These curves do match reasonably well for small length ratios. However, as can be seen in the figures, for length ratios nominally greater than 0.5, there is a constant error in the calculated curves (assuming that the measured curves contain the correct values). This error is greatest for the lowest Mach numbers, and decreases as the Mach number increases, until M = 1.5, when the error begins to increase once again. The calculated C_D tends to overestimate the measured C_D in the subsonic regime, and underestimate the measured C_D in the supersonic regime (except for M = 1.5, where it overestimates the measured values). The reason for this error is as yet to be discovered; therefore, only these two figures have been presented as representative of the curves obtained for all of the diameter ratios and Mach numbers.

IV. CONCLUSIONS

The purpose of this study has been to examine the drag data of a blunt cylinder / cylindrical probe configuration to determine various characteristics of the flow past the configuration. The configuration is important because of the reduction of drag of the cylinder/probe combination over the blunt cylinder alone. This particular set of data is significant because it represents the first in-depth study of the cylinder/probe combination in the transonic regime.

Most of the results were as expected. C_D decreased as l/d_2 increased, due to the decreased stagnation pressure of the probe wake. In the subsonic tests, C_D reached a minimum and then gradually increased, as the flow over the probe transitioned from the open to the closed mode. In the supersonic tests, the increase in C_D was rather abrupt, due to a sudden mode transition, as observed in other experiments. A hysteresis condition in C_D, and hence in the flow mode, was observed in the supersonic tests, in agreement with earlier results. As d_1/d_2 increased from 0 to 1, C_D first decreased due to the increasing size of the wake. C_D reached a minimum and then increased, due to the increasing influence of the flow stagnating on the probe face.

Most of the variations in C_D with Mach number were also expected. In all cases, C_D increased as M increased from 0.95 to 1.1, due to the phenomenon of transonic drag

rise. For the smaller length ratios, C_D increased as M increased, which is essentially how a blunt body behaves. For the two smaller diameter ratios, C_D decreased as M increased above M = 1.1, resembling the well-documented behavior of streamlined bodies. The probe length at which the transition from blunt-body to streamlined-body behavior in the supersonic regime occurred was noted, roughly at l/d_2 = 0.9. In most cases where C_D rose with increasing M where there were no significant changes in the flowfield, the rise in C_D was attributed to an increase in stagnation pressure with increasing M.

Two unexpected results were also observed: a decrease in C_D for certain ranges of probe length and diameter ratios as M increased from 0.8 to 0.95, and an increase in C_D for certain ranges of probe length and diameter ratios as M increased from 1.1 to 1.2. These results were attributed to the variation of critical probe length ratio (the probe length ratio at which the flow transitioned from one mode to the other) with Mach number. As M increases in the subsonic range, $(l/d_2)_{cr}$ increases, effectively shortening the probe and causing the flow to transition to the lower-drag open mode. In the supersonic regime, since $(l/d_2)_{cr}$ decreases with increasing M, this behavior is reversed. The ranges of length and diameter ratios for which this behavior were noted, roughly $1.5 < l/d_2 < 2.5$ for the subsonic cases, $1.8 < l/d_2 < 2.2$ for the supersonic

cases, and $0.2 < d_1/d_2 < 0.5$ for both the subsonic and supersonic cases.

An attempt was made to compute C_D for the cylinder/probe configuration from the probe face and cylinder face pressures and an estimate of the cylinder skin friction drag. These values only matched the measured C_D's within experimental error in some cases. The cause of the discrepancy has not been determined.

This experiment provided a significant piece to the cylinder/probe drag puzzle. The behavior of this configuration in the transonic regime has now been documented to a certain degree. However, as with almost all experiments, the knowledge gained is not complete. The most important pieces still missing are data for a wider range of probe length and diameter ratios. More extensive LDV measurements of the flowfield, as well as flow visualizations in the transonic regime, would be extremely useful in correlating the behavior of the flowfield and the drag experienced by the cylinder/probe configuration. Much remains to be learned about this extremely complex, but also rather intriguing, problem in fluid dynamics.

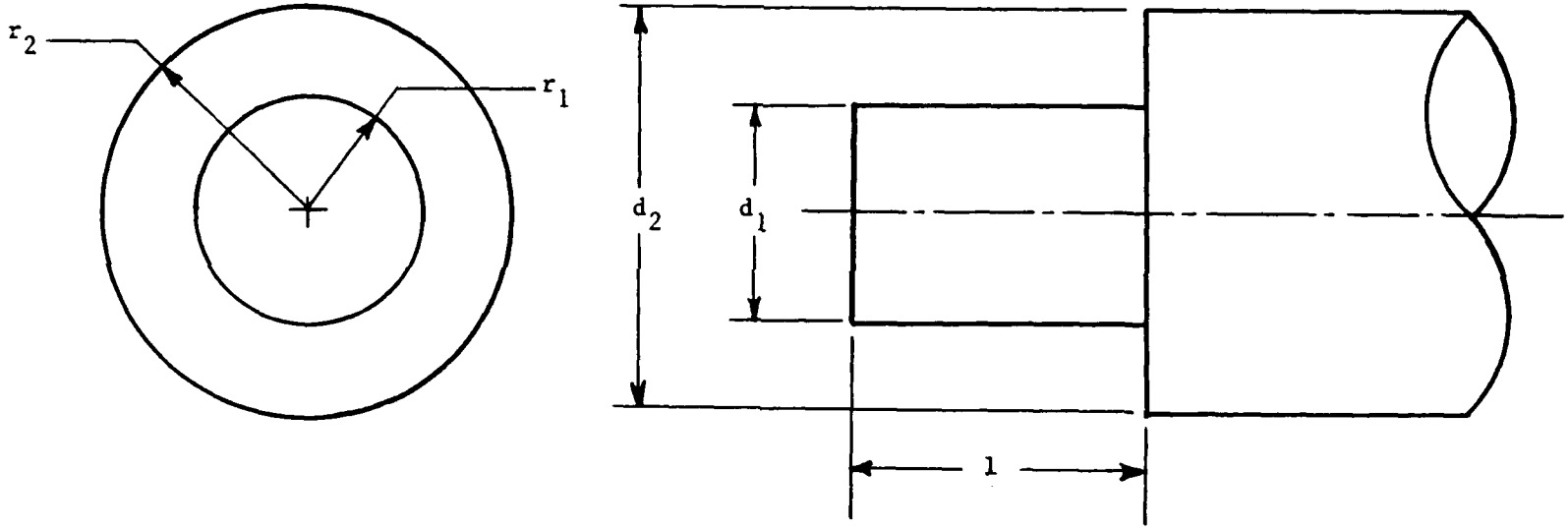

Figure 1. Cylinder-Probe Configuration

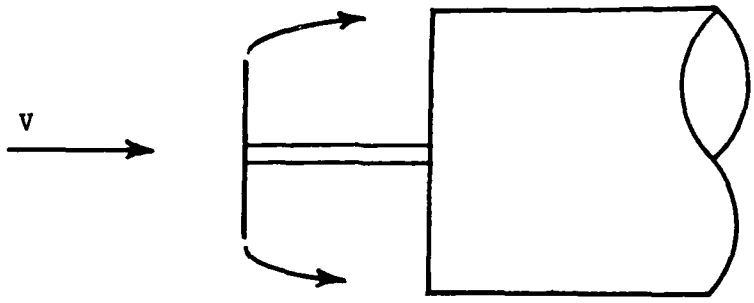

a. Disc

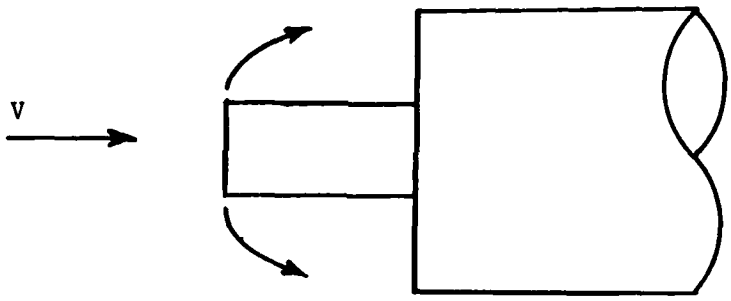

b. Cylindrical Probe

Figure 2. Flow Separation Patterns

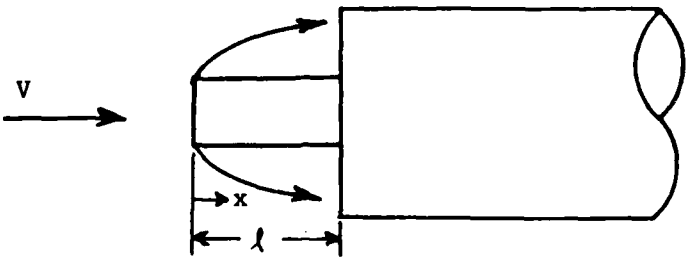

a. Open

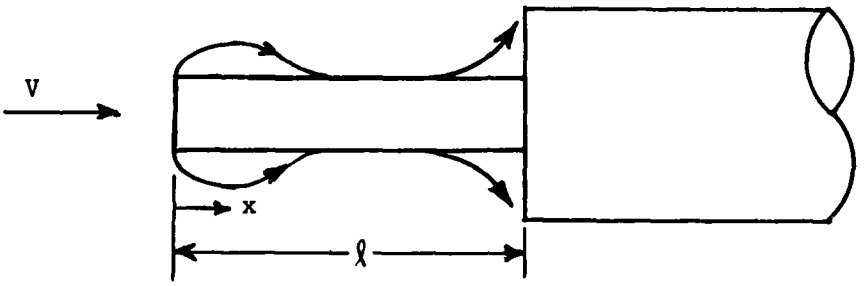

b. Closed

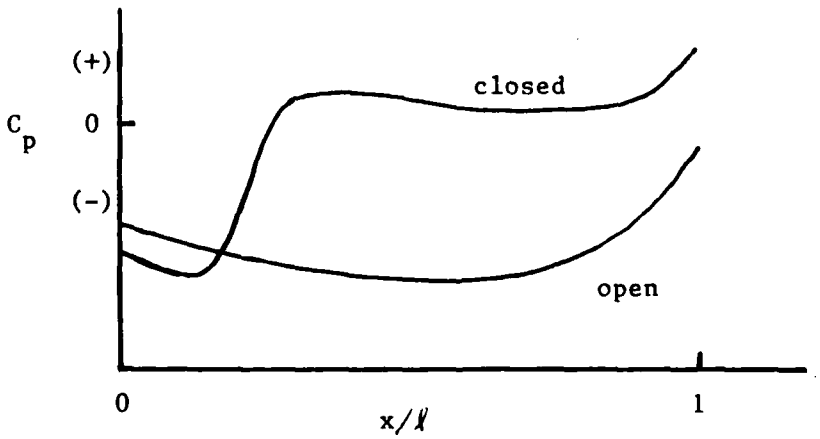

c. Pressure distributions

Figure 3. Flow Mode Comparisons

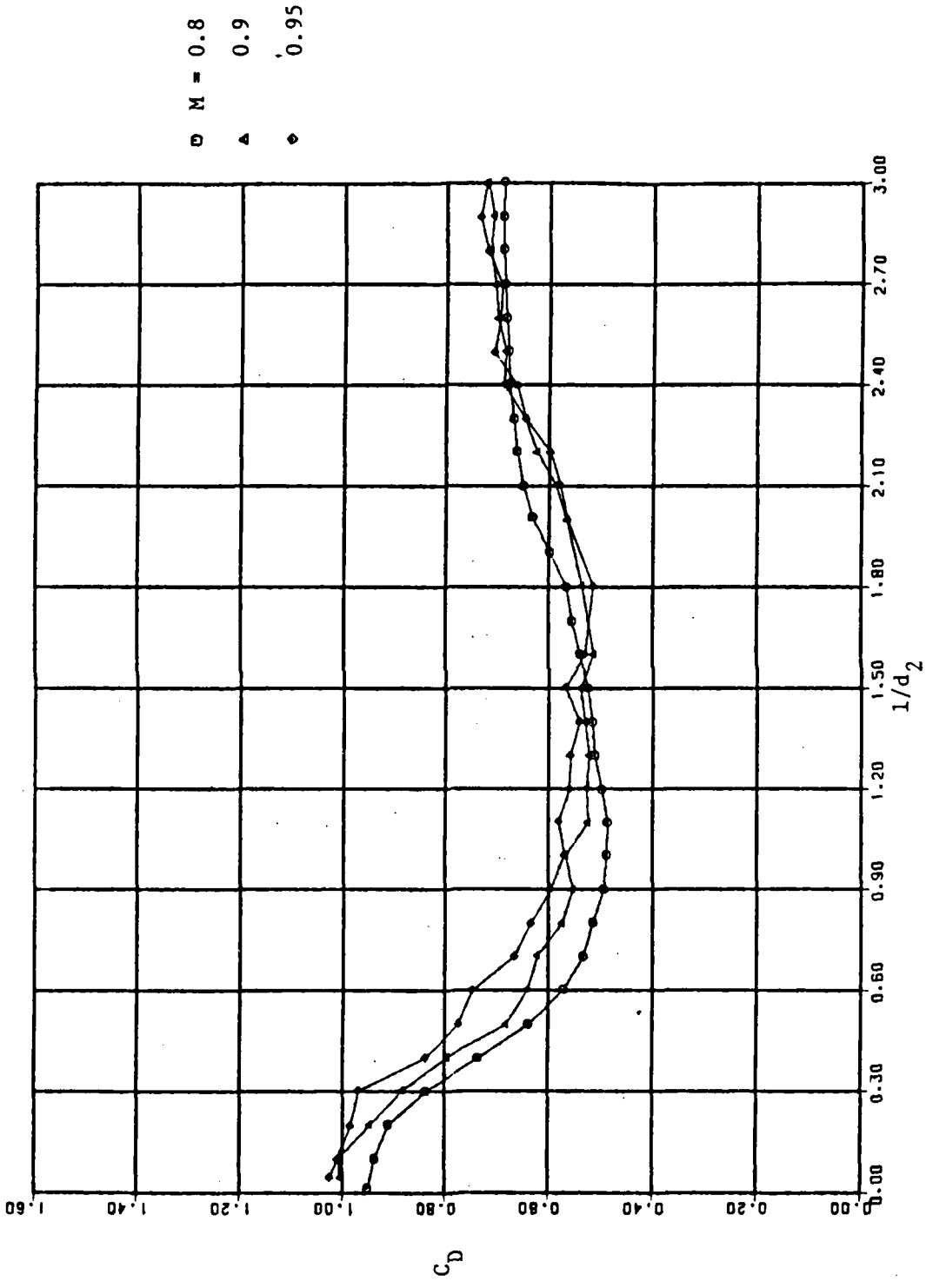

Figure 4a. Variation of C_D with Probe Length Ratio: $d_1/d_2 = 0.248$

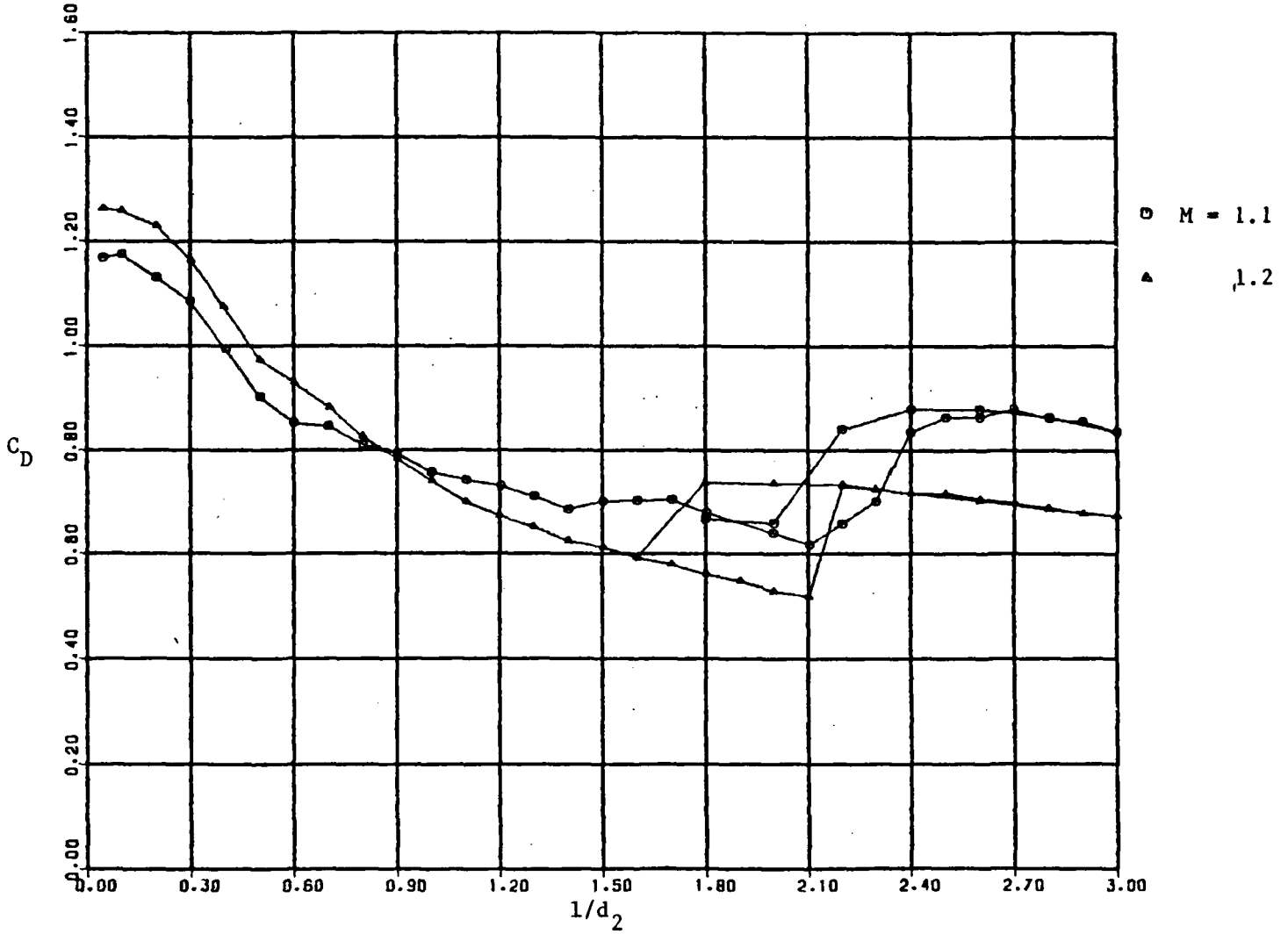

Figure 4b. Variation of C_D with Probe Length Ratio: $d_1/d_2 = 0.248$

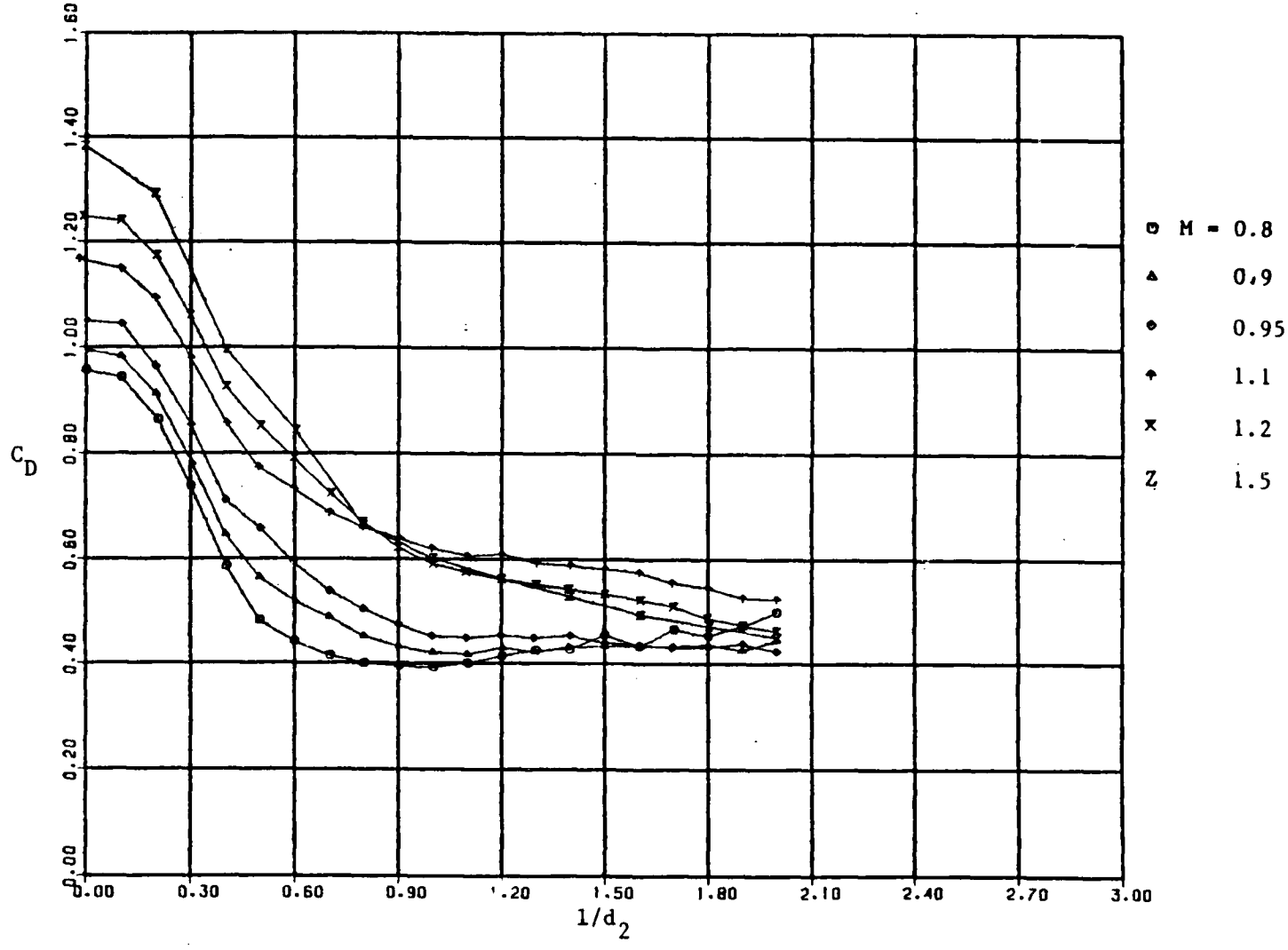

Figure 4c. Variation of C_D with Probe Length Ratio: $d_1/d_2 = 0.368$

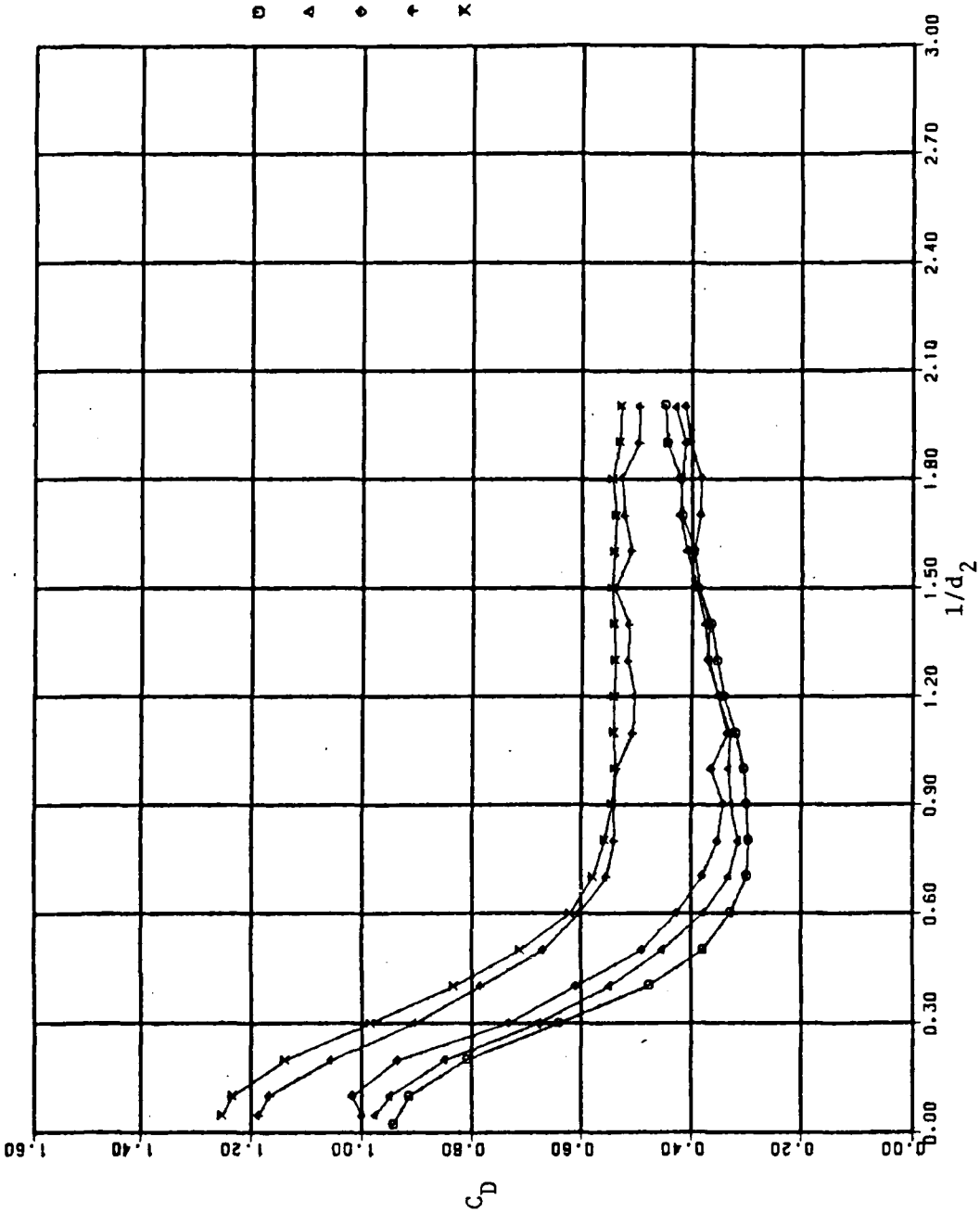

Figure 4d. Variation of C_D with Probe Length Ratio: $d_1/d_2 = 0.45$

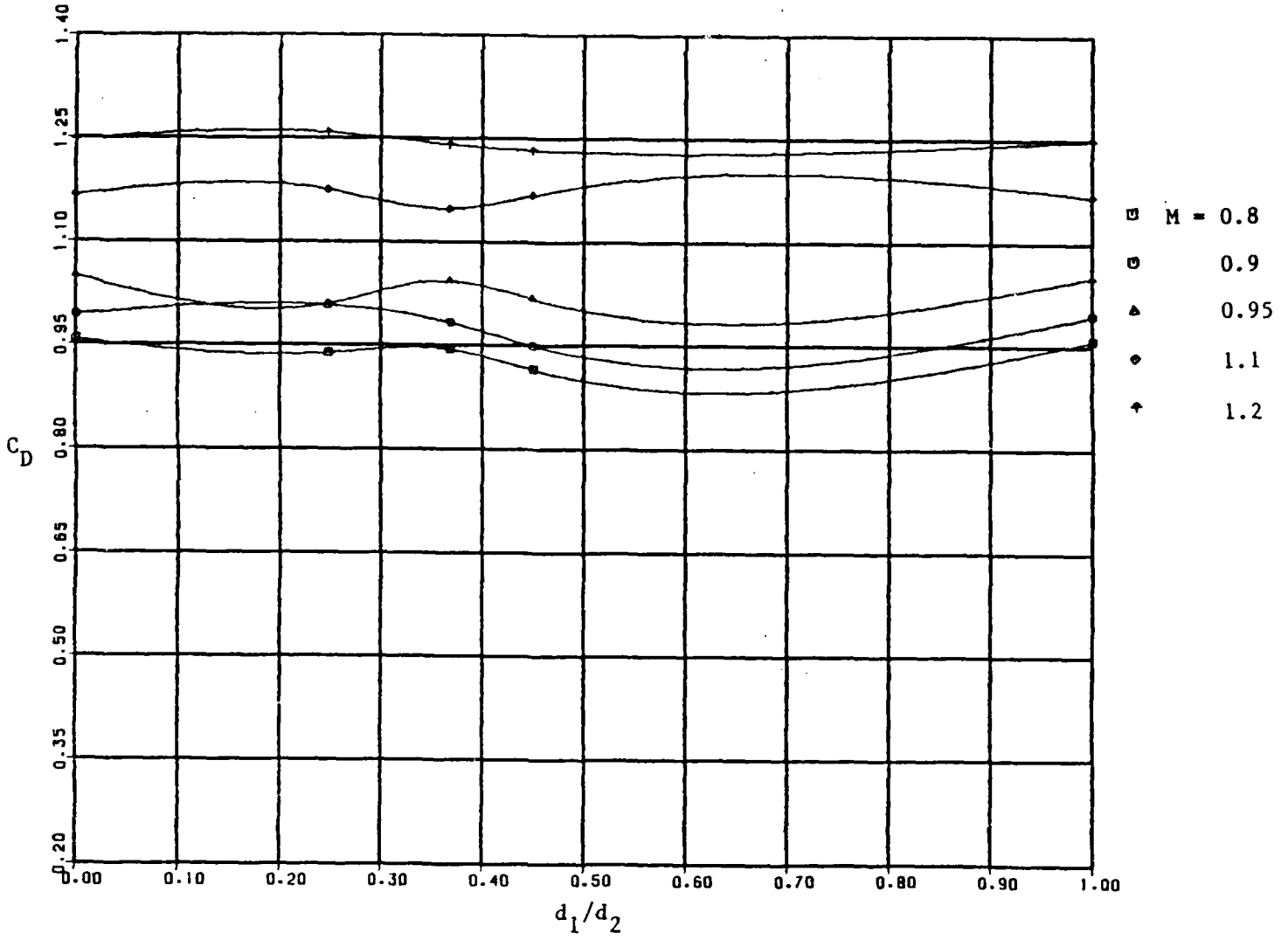

Figure 5a. Variation of C_D with Diameter Ratio: $1/d_2 = 0.1$

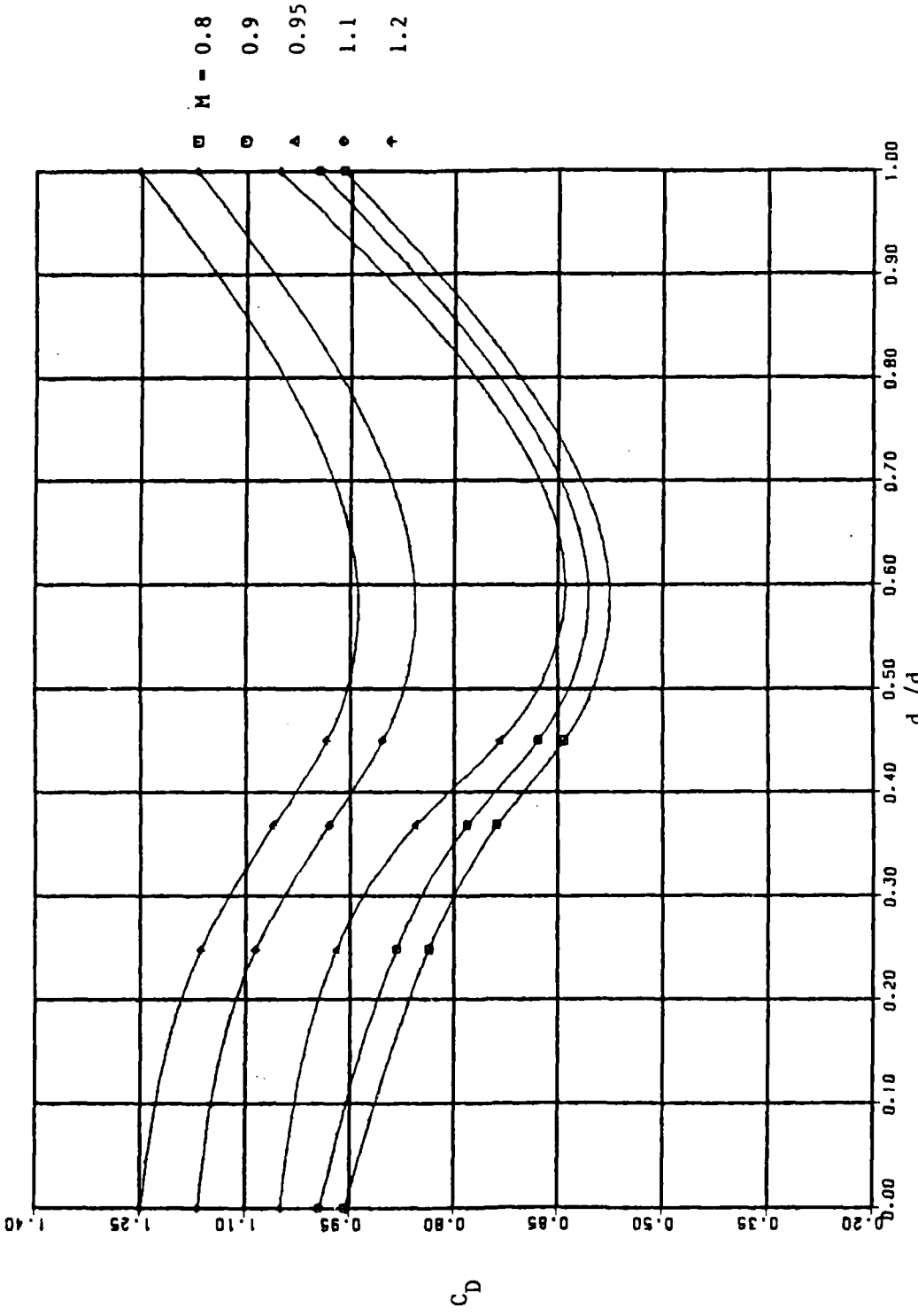

Figure 5b. Variation of C_D with Diameter Ratio: $l/d_2 = 0.3$

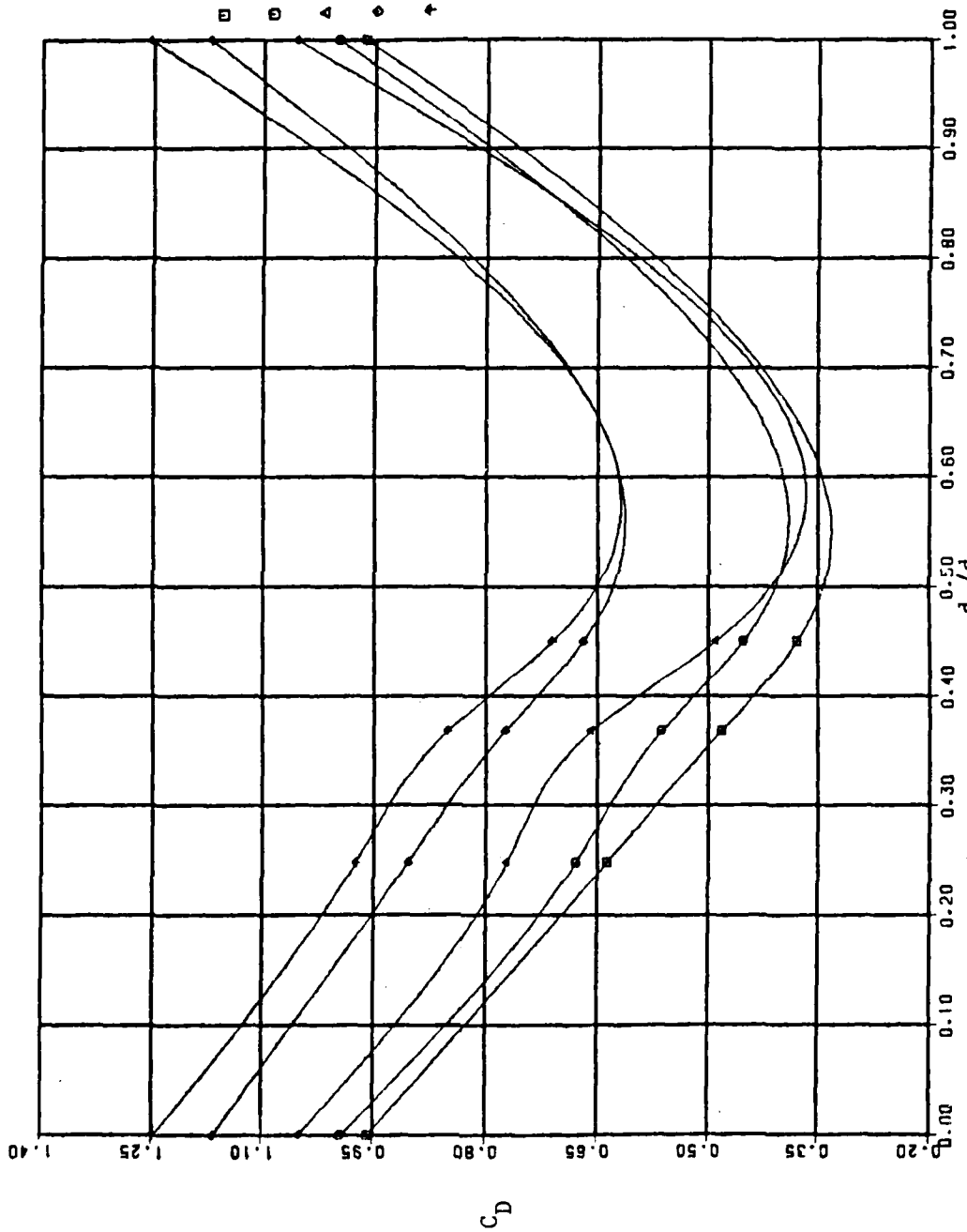

Figure 5c. Variation of C_D with Diameter Ratio: $1/d_2 = 0.5$

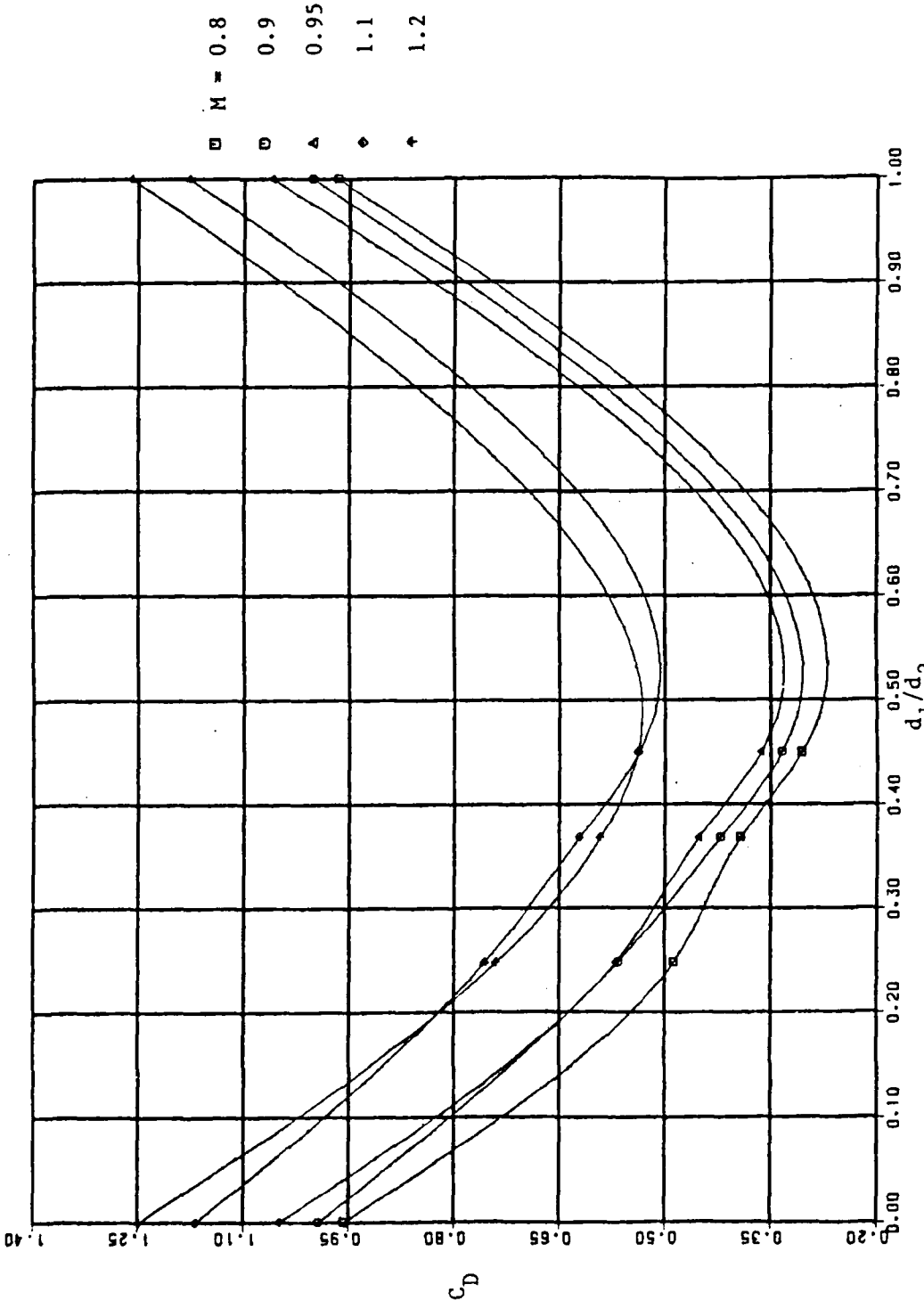

Figure 5d. Variation of C_D with Diameter Ratio: $1/d_2 = 1.0$

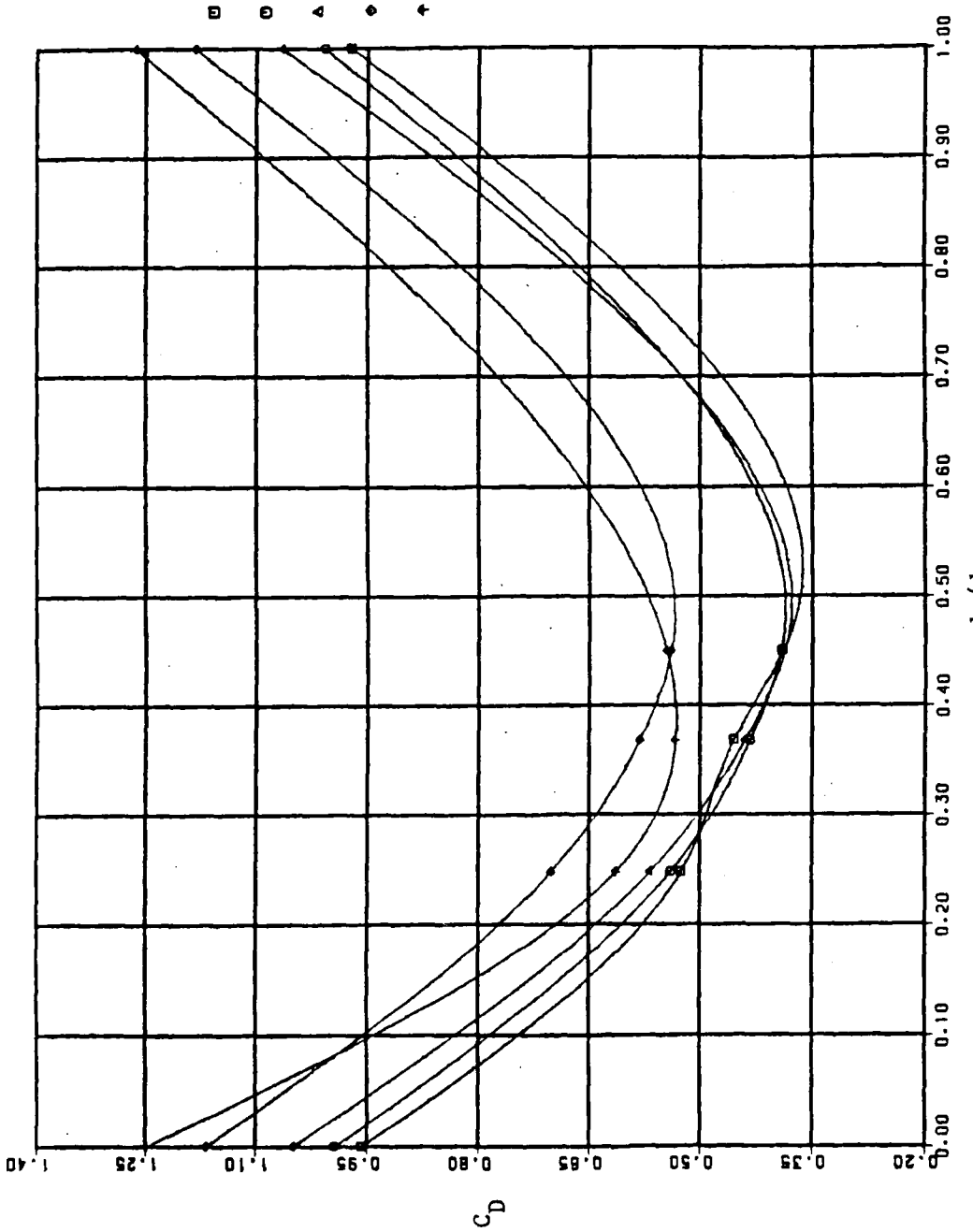

Figure 5e. Variation of C_D with Diameter Ratio: $1/d_2 = 1.5$

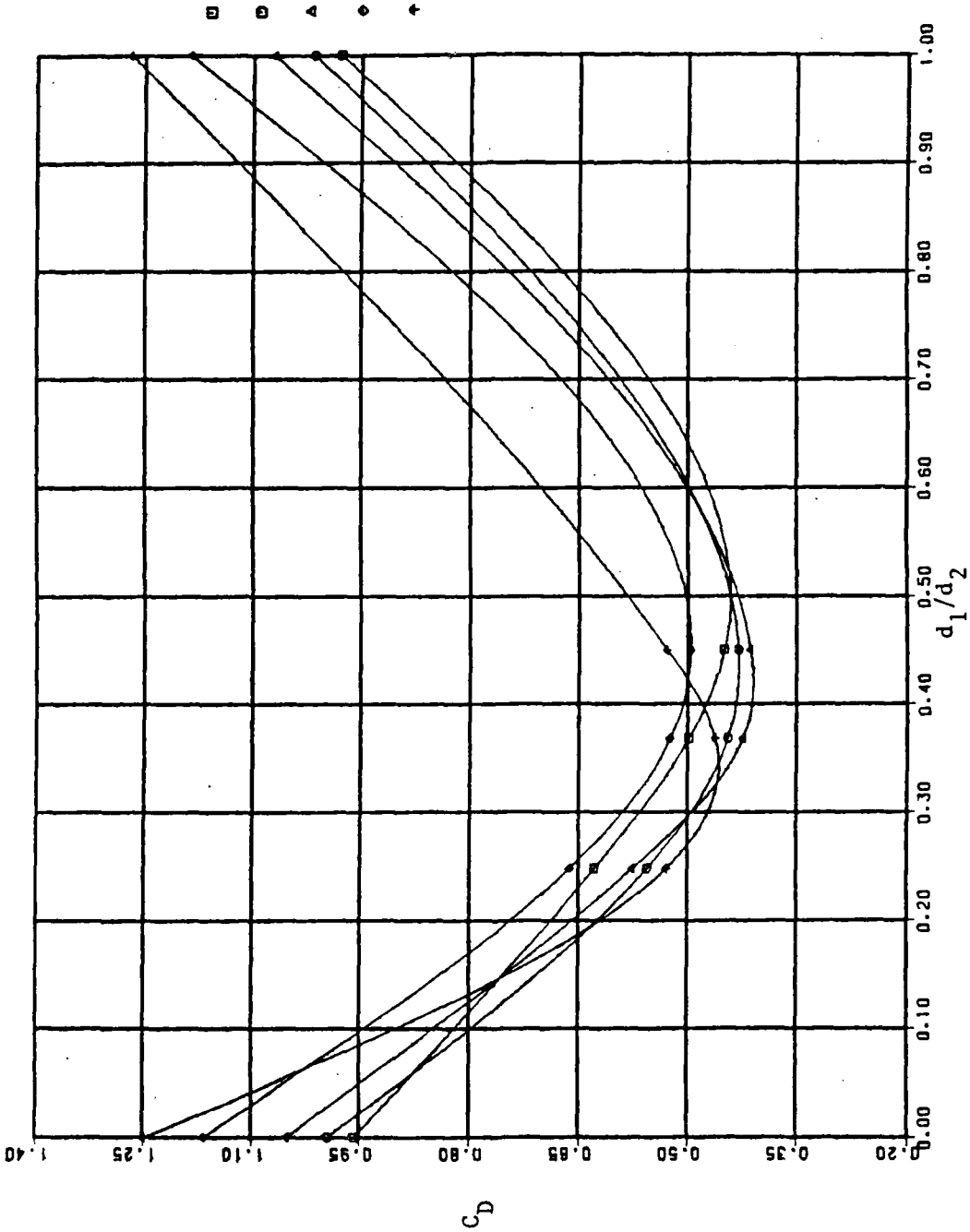

Figure 5f. Variation of C_D with Diameter Ratio: $l/d_2 = 2.0$

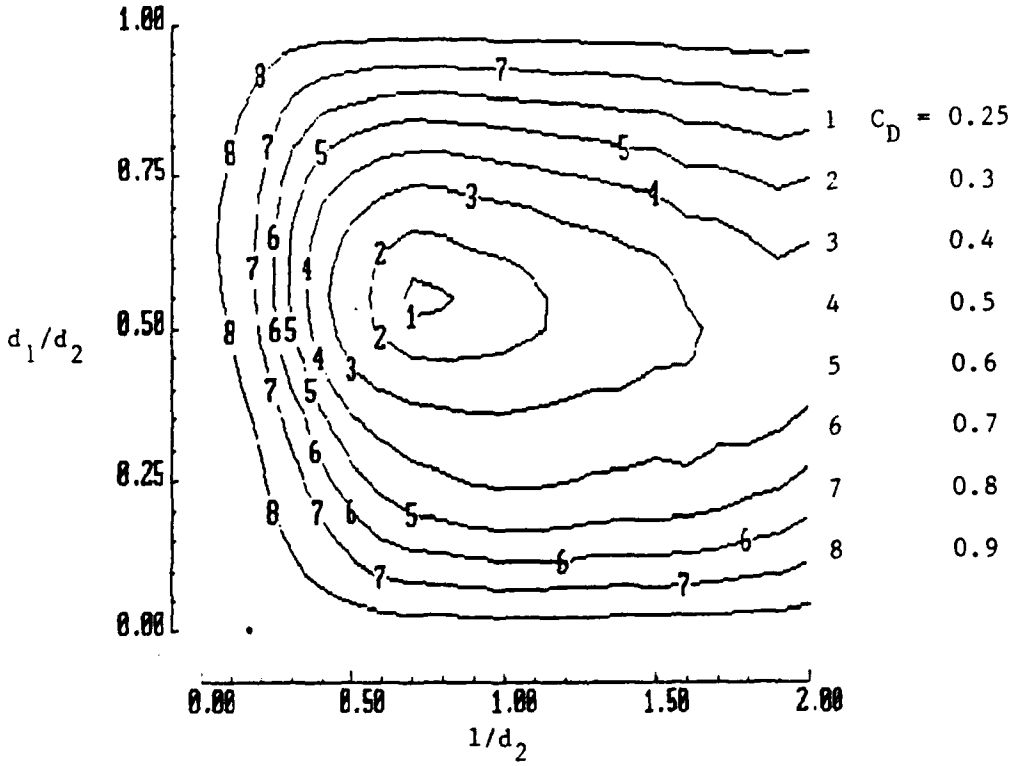

Figure 6a. Drag Coefficient Contours: M = 0.8

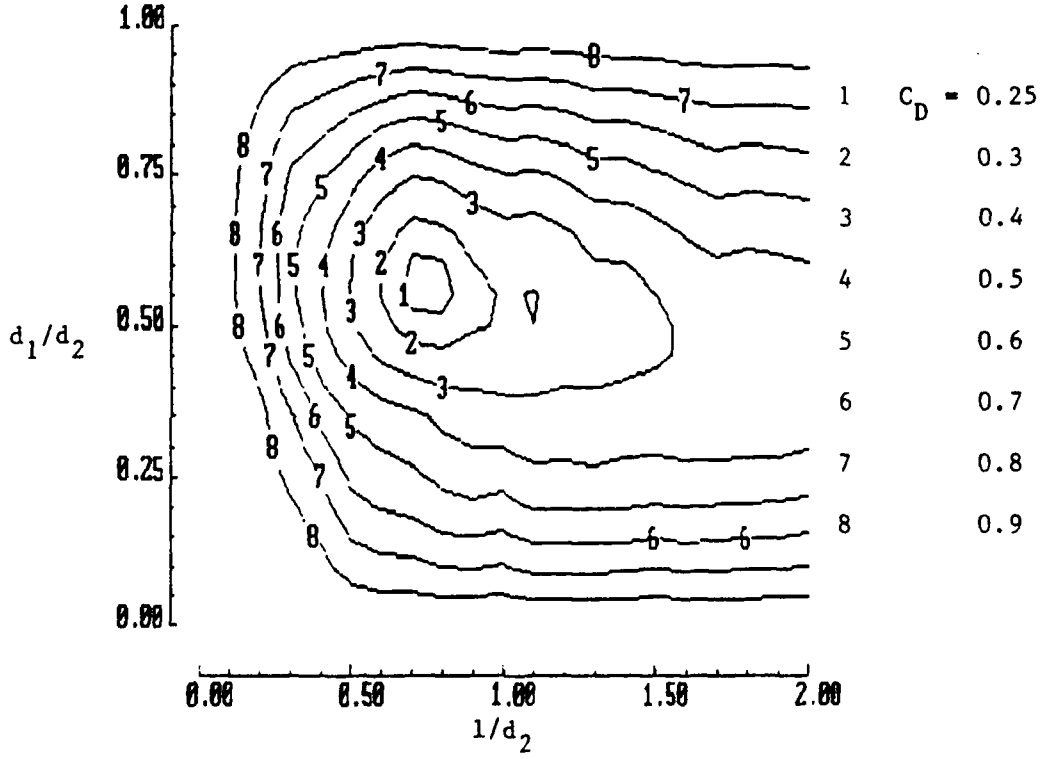

Figure 6b. Drag Coefficient Contours: M = 0.9

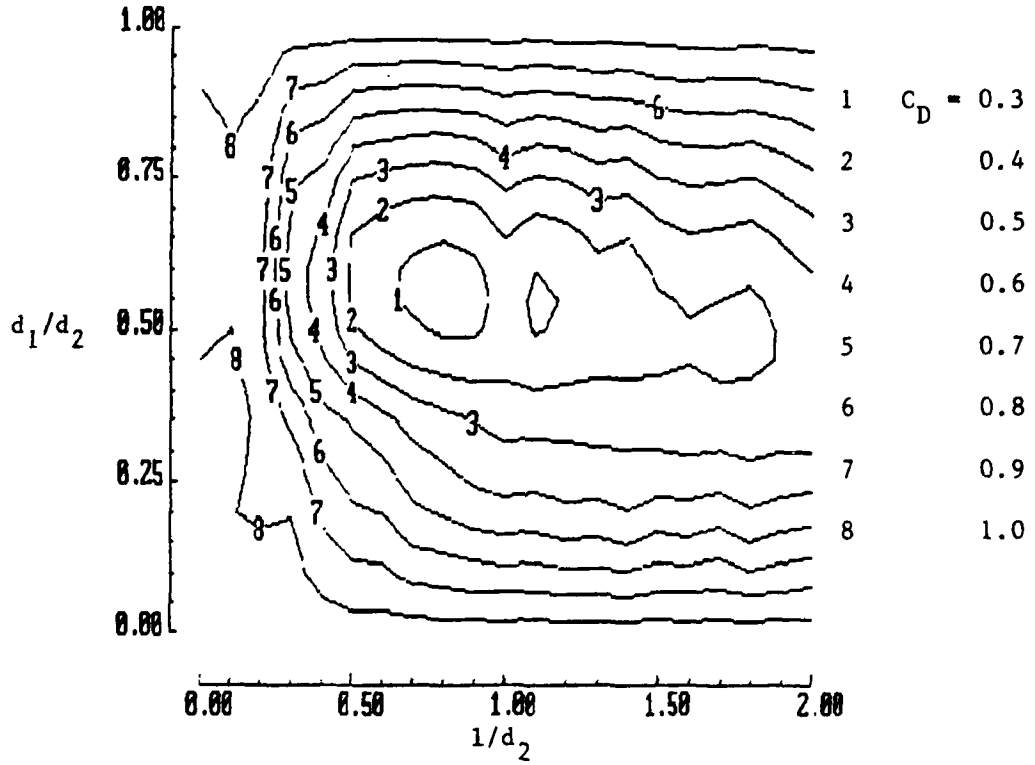

Figure 6c. Drag Coefficient Contours: M = 0.95

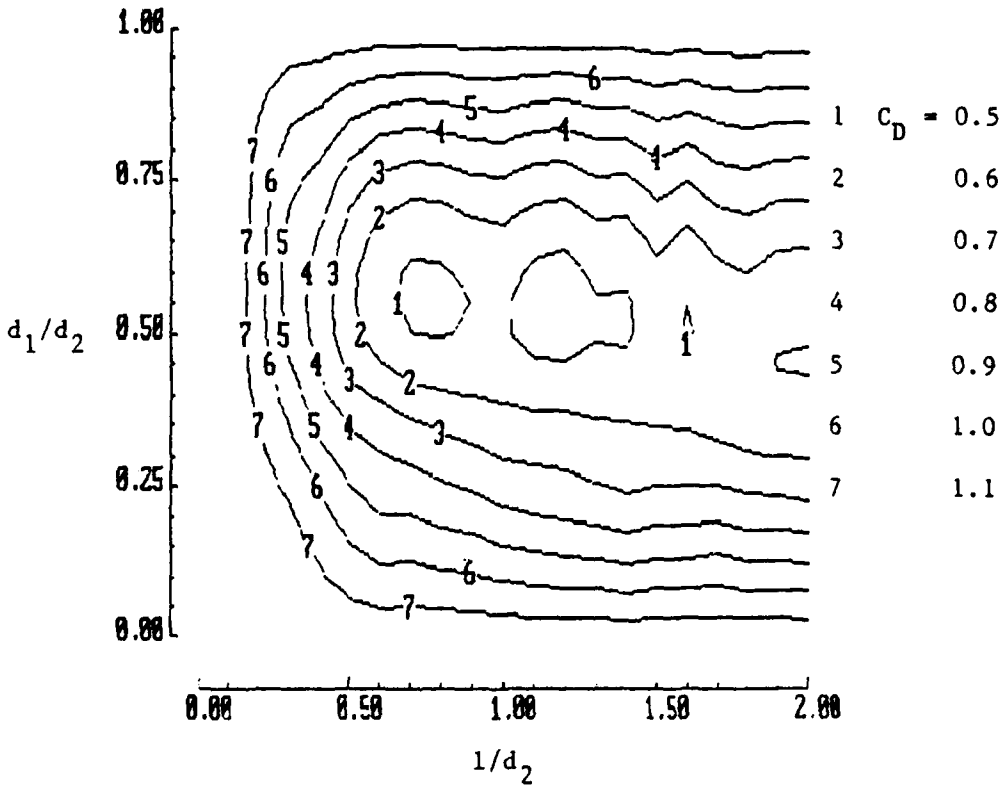

Figure 6d. Drag Coefficient Contours: M = 1.1

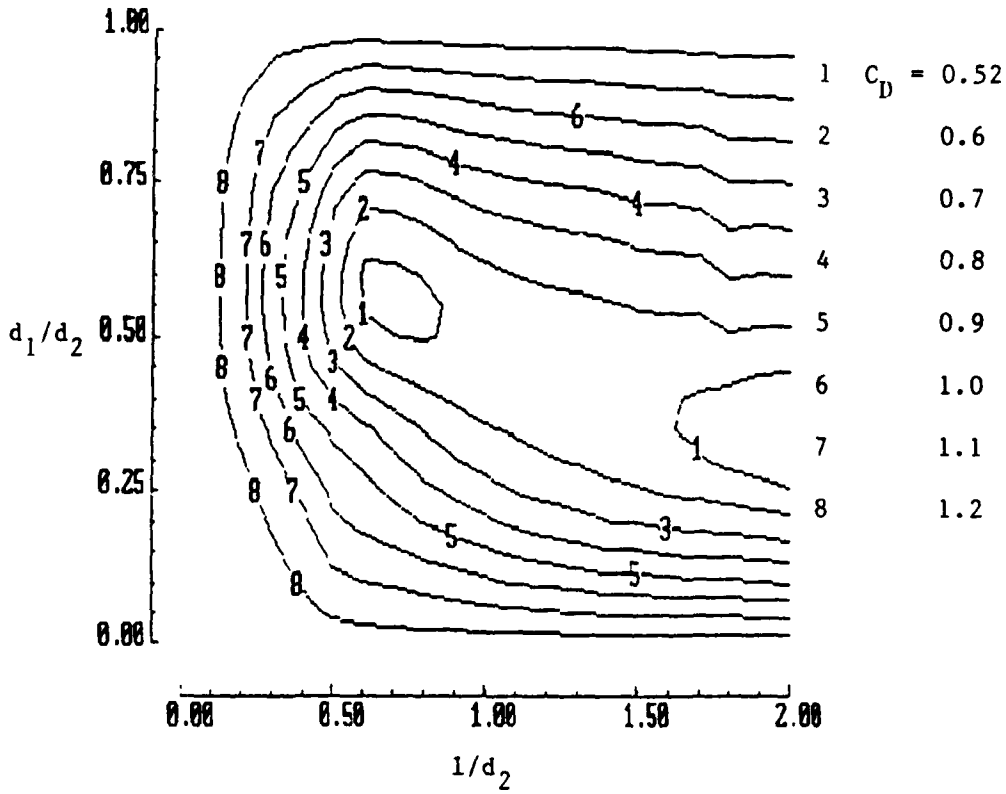

Figure 6e. Drag Coefficient Contours: M = 1.2

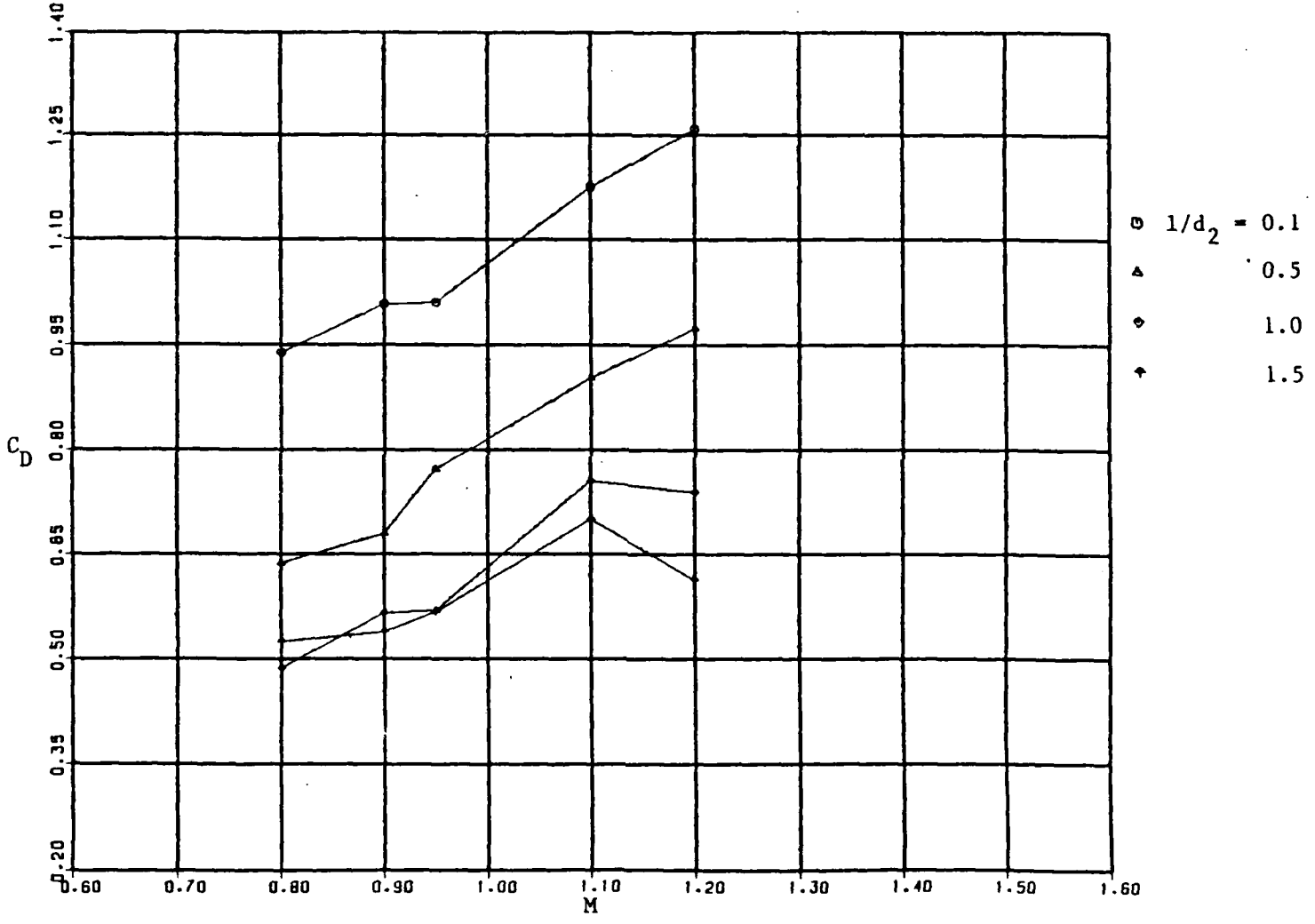

Figure 7a. Variation of C_D with Mach Number: d_1/d_2 = 0.248

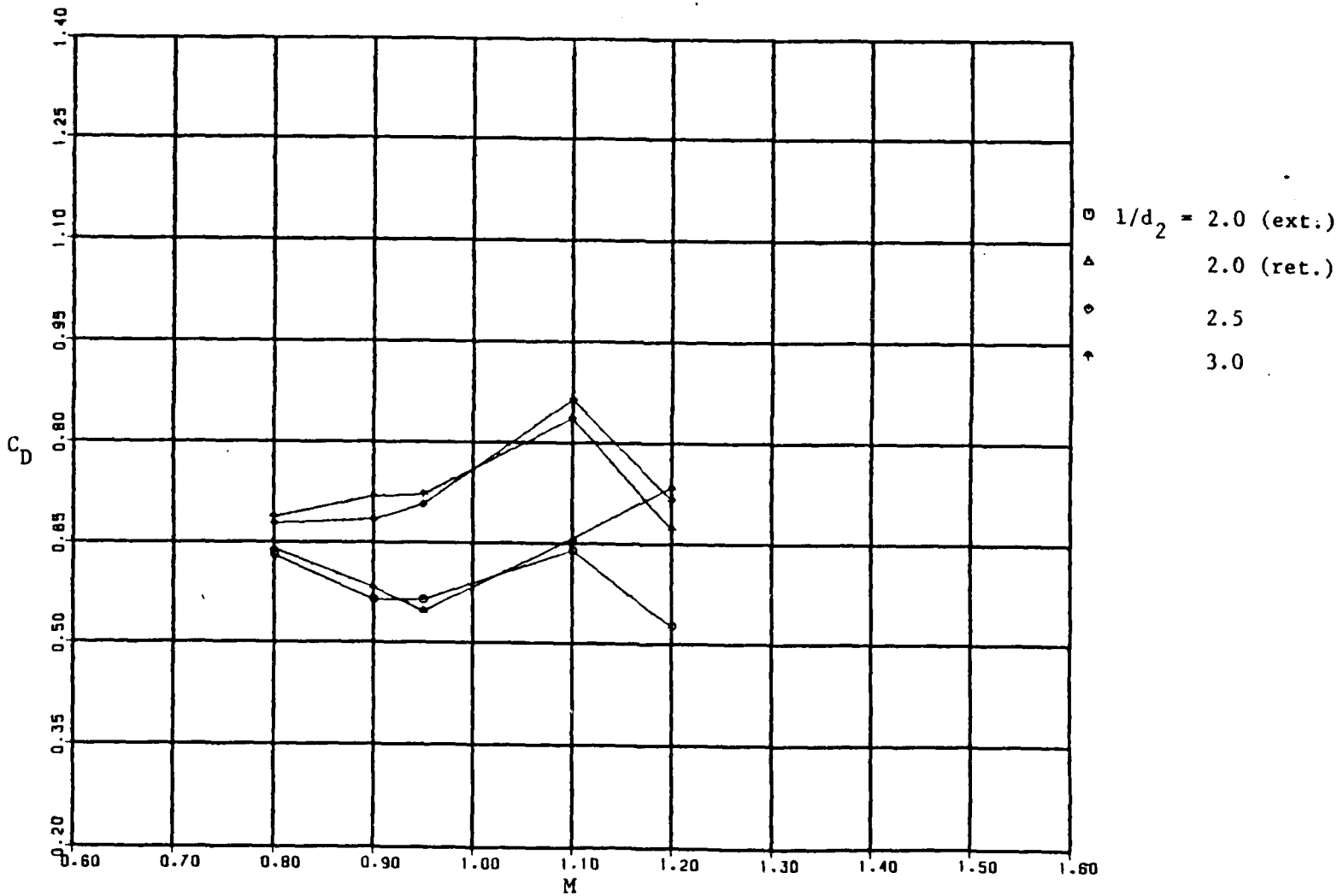

Figure 7b. Variation of C_D with Mach Number: $d_1/d_2 = 0.248$

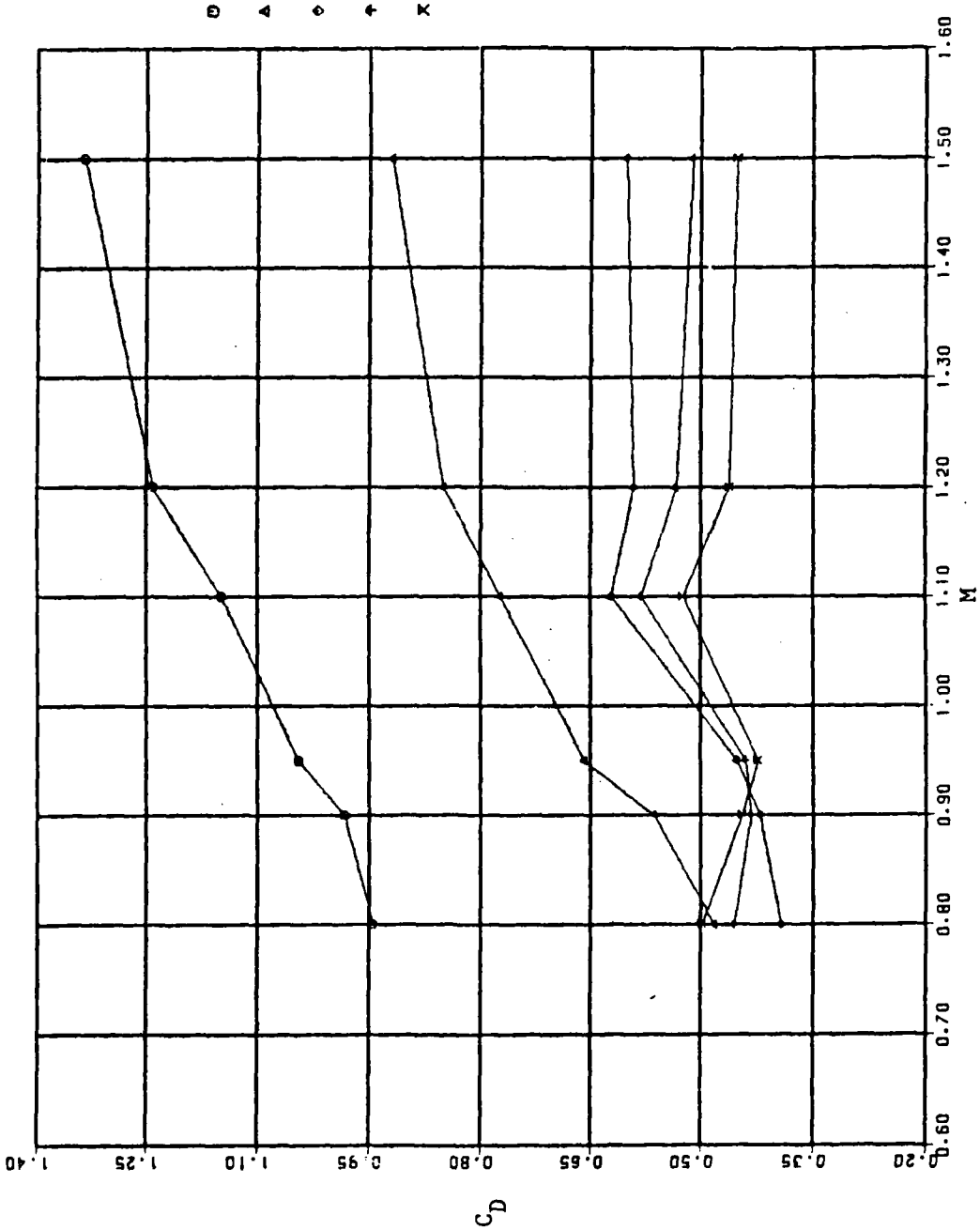

Figure 7c. Variation of C_D with Mach Number: d_1/d_2 = 0.368

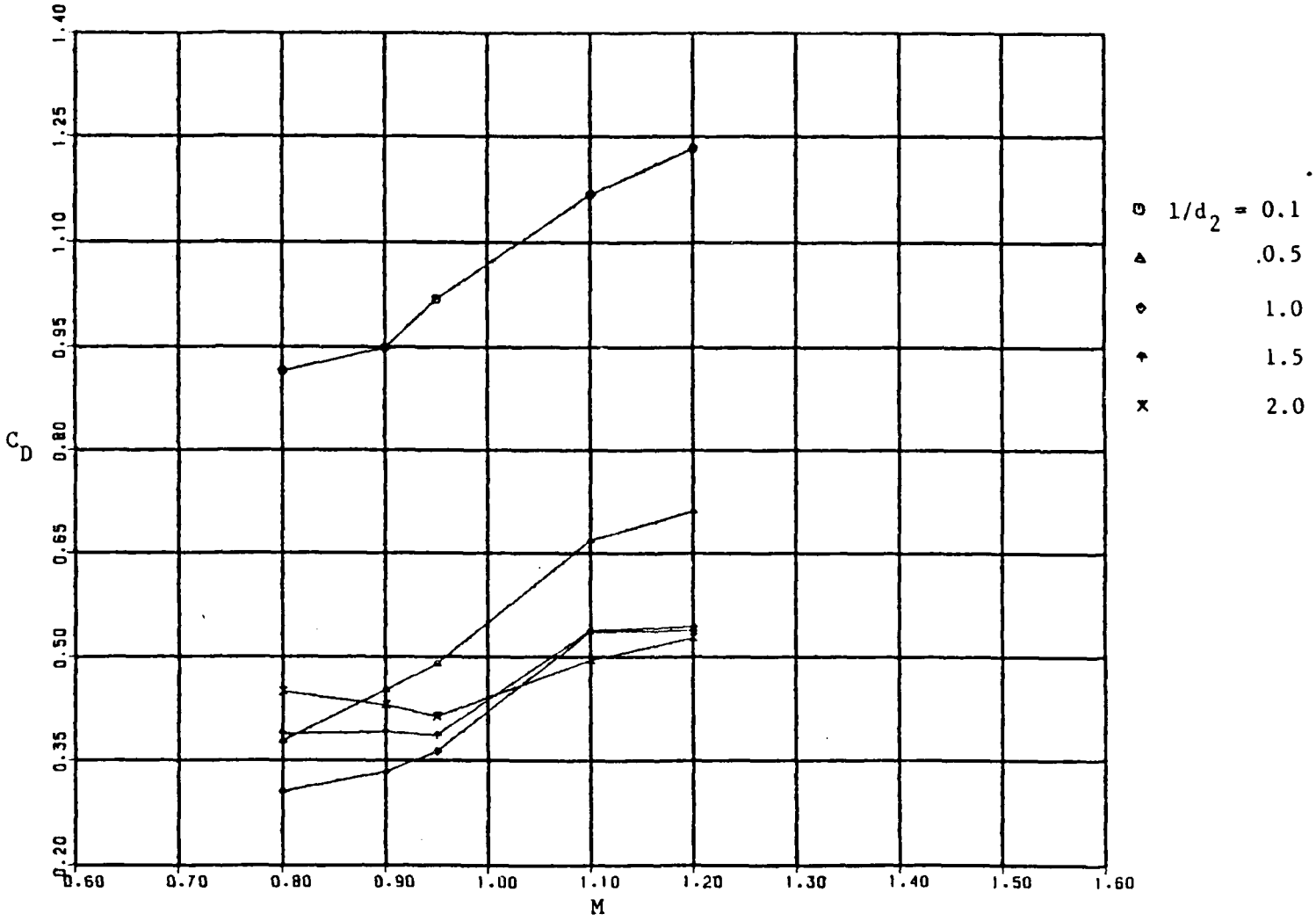

Figure 7d. Variation of C_D with Mach Number: $d_1/d_2 = 0.45$

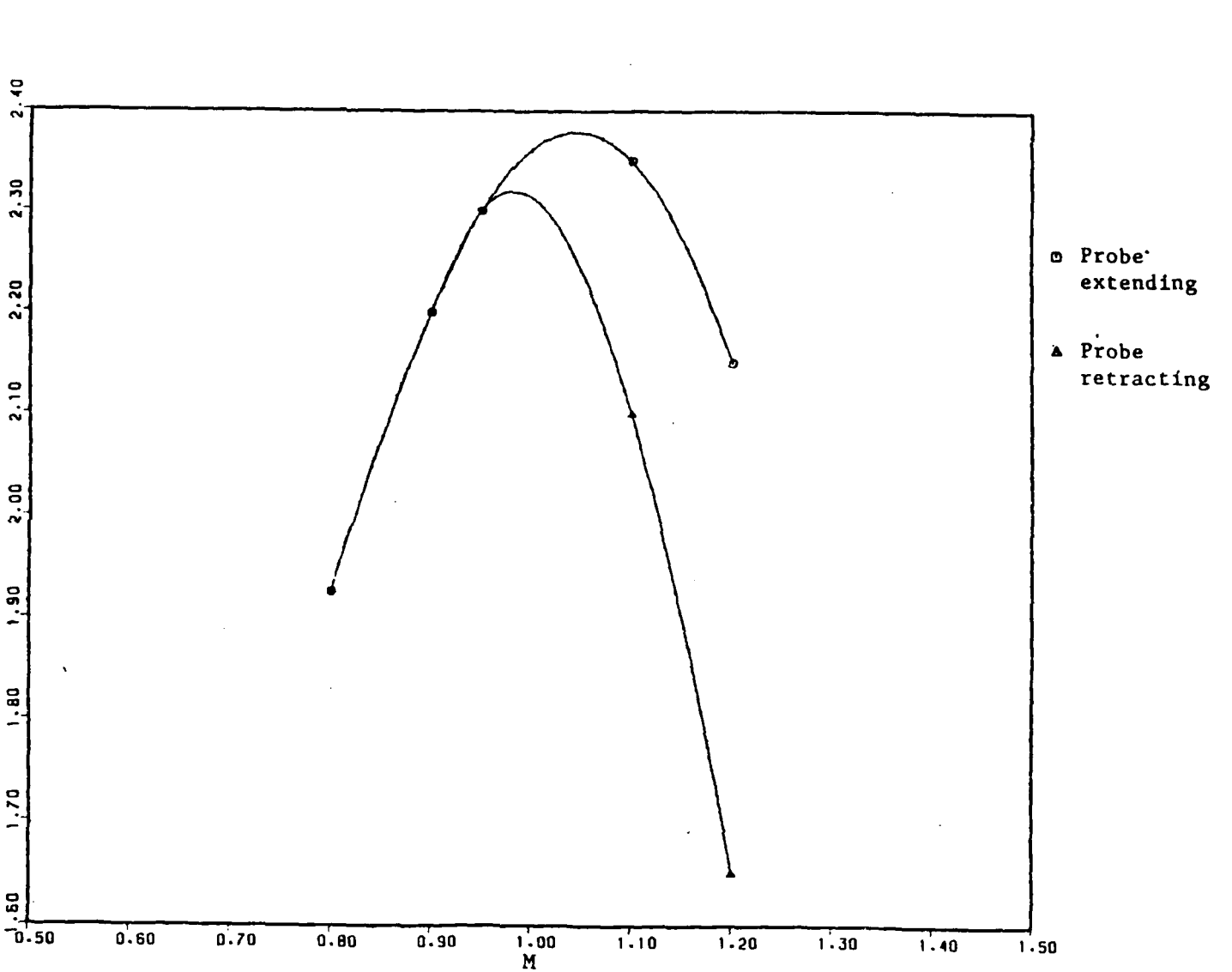

Figure 8. Variation of Critical Probe Length Ratio with Mach Number

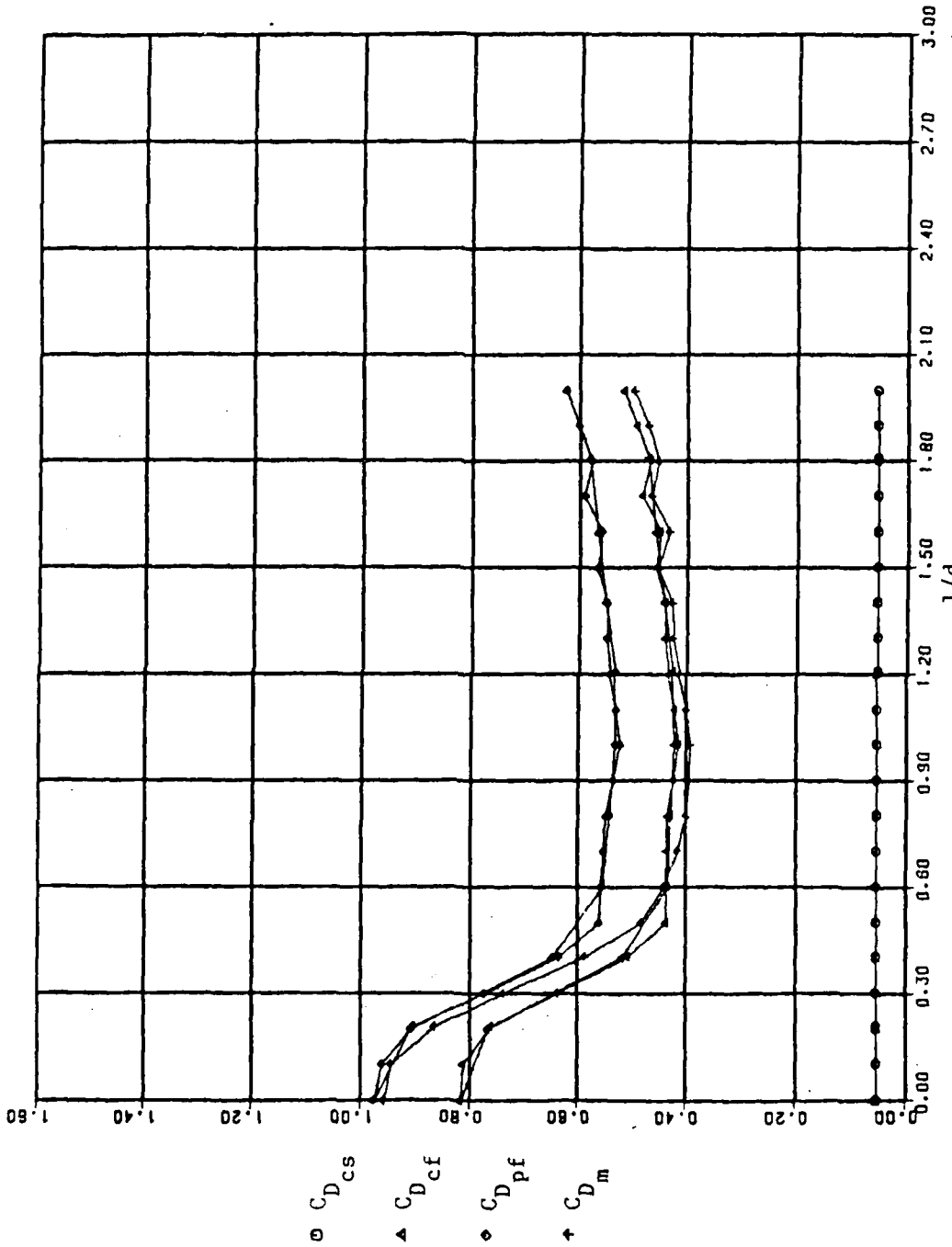

Figure 9a. Computed and Measured Drag Coefficients: $d_1/d_2 = 0.368$, M = 0.8

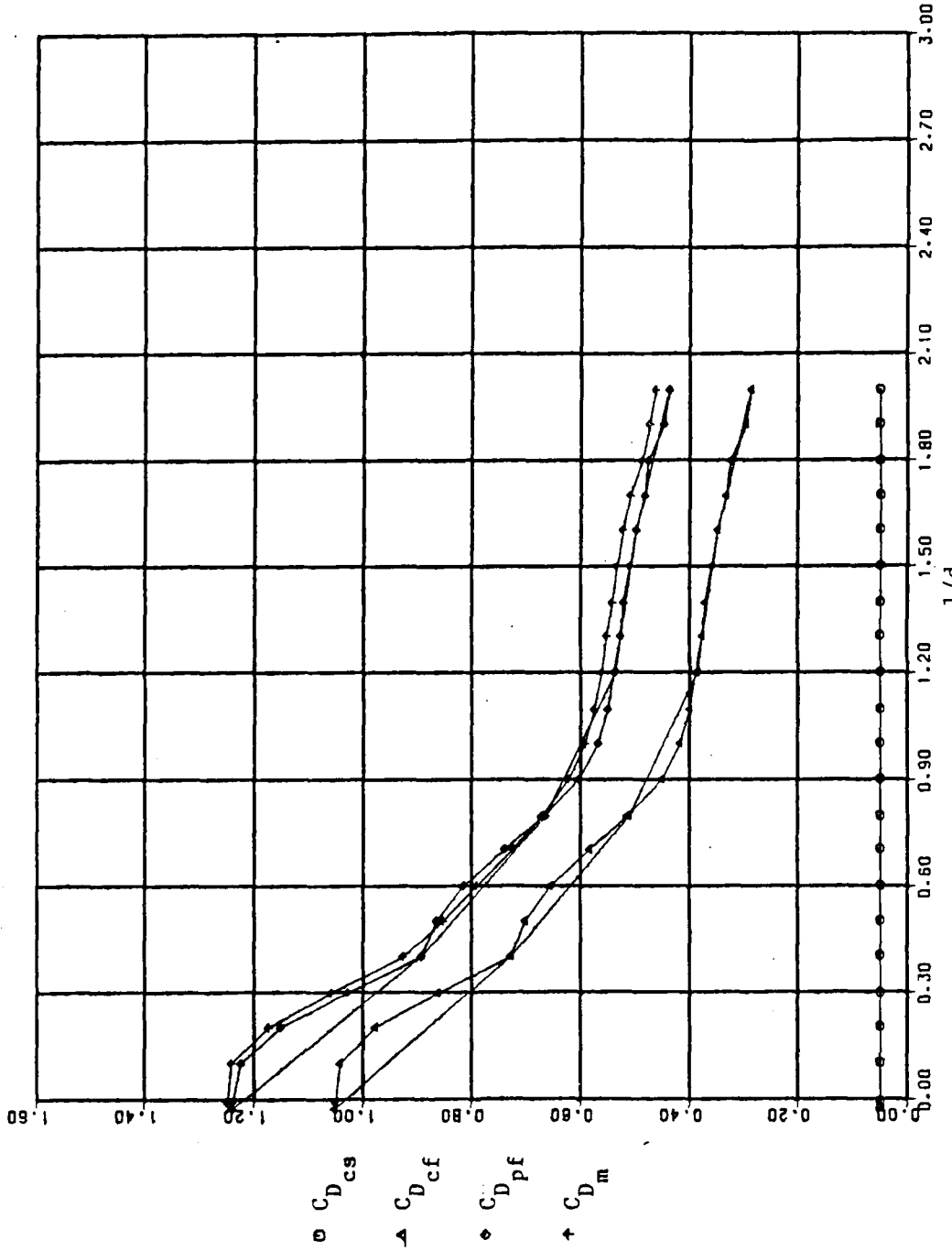

Figure 9b. Computed and Measured Drag Coefficients: $d_1/d_2 = 0.368$, M = 1.2

REFERENCES

[1]Koenig, K., and Roshko, A., "An experimental study of geometrical effects on the drag and flow field of two bluff bodies separated by a gap," Journal of Fluid Mechanics, Vol. 156, 1985, pp. 167-204.

[2]Spooner, S. H., "Static Longitudinal Stability Characteristics of a Series of 90-Millimeter Artillery Shells at Mach Numbers of 0.8, 0.9, 1.0, and 1.2," NACA RM SL 56D27, May 1956.

[3]Beastall, D., and Turner, J., "The Effect of a Spike Protruding in Front of a Bluff Body at Supersonic Speeds," ARC R&M No. 3007, 1957.

[4]Saunders, W. S., "Apparatus for Reducing Linear and Lateral Wind Resistance in a Tractor-Trailer Combination Vehicle," U.S. Patent No. 3,241,876, 1966.

[5]Buckley, F. T., Jr., and Sekscienski, W. S., "Comparisons of Effectiveness of Commercially Available Devices for the Reduction of Aerodynamic Drag on Tractor-Trailers," SAE 750704, 1975.

[6]Haupt, B. F., and Koenig, K., "Aerodynamic Effects of Probe-Induced Flow Separation on Bluff Bodies at Transonic Mach Numbers", Journal of Spacecraft and Rockets, to be published.

[7]Koenig, K., "Transonic Merging Separated Flows," Final Report, AFOSR Grant 83-0179, July 1984.

[8]Eiffel, G., The Resistance of the Air and Aviation, 2nd ed., Hunsaker, J. C., (translator), Constable and Co., London, 1913.

[9]Morel, T., and Bohn, M., "Flow Over Two Circular Discs in Tandem," Transactions of the ASME, Journal of Fluids Engineering, March 1980, pp. 104-111.

[10]Koenig, K., Griffin, L., and Vincent, L., "An Experimental Study of an Axisymmetric Cavity-Like Flow," AIAA Journal, to be published.

[11]Charwat, A. F., Roos, J.N., Dewey, F. C., Jr., and Hite, J. A., "An Investigation of Separated Flows -- Part I: The Pressure Field," Journal of the Aerospace Sciences, June 1961, pp. 459-470.

[12]Johannesen, N. H., "Experiments on Supersonic Flow Past Bodies of Revolution with Annular Gaps of Rectangular Section," Philosophical Magazine, Ser. 7, Vol. 46, No. 372, January 1955, pp. 31-39.

[13]Roshko, A., "Some Measurements of Flow in a Rectangular Cutout," NACA TN 3488, August 1955.

[14]White, F. M., "An Analysis of Axisymmetric Turbulent Flow Past a Long Cylinder," Transactions of the ASME, Journal of Basic Engineering, March 1972, pp. 200-204.

[15]Chapman, D. R., and Kester, R. H., "Turbulent Boundary-Layer and Skin-Friction Measurements in Axial Flow Along Cylinders at Mach Numbers Between 0.5 and 3.6," NACA TN 3097, March 1954.

[16]Hoerner, S. F., Fluid-Dynamic Drag, Hoerner Fluid Dynamics, Brick Town, NJ, 1965.

[17]Stoney, W. E., Jr., "Collection of Zero-Lift Drag Data on Bodies of Revolution from Free-Flight Investigations," NACA TN 4201, January 1958.